Improving 3D Reconstruction using Shape from Shading by Applying Optimal Thresholding and Histogram Processing

by

Ms. Vadeerat Rinsurongkawong

Submitted in Partial Fulfillment of
The Requirements for the Degree of
Master of Science
In Information Technology
Assumption University

March, 2002

Improving 3D Reconstruction using Shape from Shading by Applying Optimal Thresholding and Histogram Processing

by

Ms. Vadeerat Rinsurongkawong

Submitted in Partial Fulfillment of
the Requirements for the Degree of
Master of Science
in Information Technology
Assumption University

March, 2002

The Faculty of Science and Technology

Thesis Approval

Thesis Title	Improving 3D Reconstruction using Shape from Shading by Applying Optimal Thresholding and Histogram Processing
By	Ms. Vadeerat Rinsurongkawong
Thesis Advisor	Asst.Prof.Dr. Thotsapon Sortrakul
Academic Year	2/2001

The Department of Information Technology, Faculty of Science and Technology of Assumption University has approved this final report of the **twelve** credits course. **IT7000 Master Thesis**, submitted in partial fulfillment of the requirements for the degree of Master of Science in Information Technology.

Approval Committee:

(Asst.Prof.Dr. Thotsapon Sortrakul)
Advisor

(Dr. Thiraphong Charoenkhunwiwat)
Committee Member

(Dr. Jirapun Daengdej)
Committee Member

(Professor Dr. Chidchanok Lursinsap)
Representative of Ministry of
University Affairs

Faculty Approval:

(Asst.Prof.Dr. Thotsapon Sortrakul)
Director

(Asst.Prof.Dr. Pratit Santiprabhob)
Dean

March / 2001

ACKNOWLEDGEMENTS

The writer would like to thank Assistant Professor Dr. Thotsapon Sortrakul for his advice and encouragement through the course of this thesis.

She also thanks Mr. Worasing Rinsurongkawong and Mr. Chantakorn Chamsilp for the source of this studying.

Thanks Also go to Mr. Sumitr Rinsurongkawong, Mrs. Somjai Rinsurongkawong and Ms. Somchit Vachiravanichakij for their encouragement and inspiration.

LIST OF FIGURES

ABSTRACT

Shape from Shading is a technique to determine shape of the object in 3D from its gray-scale 2D image. This technique does not mimic the mechanism of the human brain but is a method applied to execute in the computing world.

Optimal Thresholding is a thresholding applied to extract or separate one objects from another in the gray-scale image.

Histogram Equalization and Histogram Specification are the histogram processing technique for enhancing the contrast of the image.

Applied Shape from shading technique in reconstructing 3D image, the result may be ambiguous because of ambiguity and darkness of 2D image.

This thesis introduces Optimal Thresholding and Histogram Processing as preprocessing to relieve the effect of darkness and ambiguity in the image before reconstructing 3D image by Shape from shading.

TABLE OF CONTENTS

CHAPTER 1 INTRODUCTION

1.1 Introduction

In reconstruction of 3D from 2D image quality of the 3D image may be deteriorated by many reasons, some of the problems are caused by the nature of the image itself.

Shape from shading is the technique introduced for recovery shape of the image in 3D from 2D image.

Optimal Thresholding is a method to extract some part of the object from gray-scale image by applying histogram in associate.

Histogram Equalization and Histogram Specification are the contrast enhancement technique used in Histogram Processing.

This thesis introduces process for 3D reconstruction by Shape from shading with applying Optimal thresholding method with Histogram Processing to get rid of or relieve some problems in the 2D image cause by some darkness or ambiguity on the 2D image which can deteriorate the generated 3D.

The thesis organizes as following: Chapter 1 is an introduction. Chapter 2 introduces concept of Shape from shading. Chapter 3 is concept of Optimal Thresholding. Chapter 4 is a Histogram Processing. Chapter 5 is proposed techniques. Chapter 6 and 7 are the experimental results and conclusion respectively. Finally Chapter 7 is bibliography.

1.2 Problem Definition

Darkness and some ambiguity parts that appear on 2D image can be the cause of ambiguity of shape in reconstructed 3D image by Shape from shading.

1.3 Objectives

The objective of the thesis is to improve the result of 3D reconstructed from Shape from shading. The ambiguity of 3D images are because of some shadow, some dark parts or some ambiguity from the 2D images. This thesis introduces the method to relieve the effect of darkness or ambiguity in 3D reconstruction using Shape from shading by applying Optimal thresholding and Histogram Processing.

1.4 Scope of Work

1. Shape from shading
   - 1.1 Studying of Shape from shading concept.
   - 1.2 Surveying of Shape from shading research and development.
   - 1.3 Implementing Shape from shading from the concept.
   - 1.4 Finding the problem of Shape from shading.
2. Optimal Thresholding
   - 2.1 Studying of Optimal Thresholding concepts.
   - 2.2 Implementing Optimal Thresholding from concept.
3. Histogram Processing
   - 3.1 Studying of Histogram Processing concepts.
   - 3.2 Studying of Histogram Equalization concept.

3.3 Studying of Histogram Specification concept.

3.4 Implementing Histogram Equalization.

3.5 Implementing Histogram Specification.

4. The proposed techniques of Improving Shape from Shading by Applying Optimal Thresholding and Histogram Processing.

3.1 Studying feasibility of the proposed techniques.

3.2 Implementing the proposed techniques.

3.3 Simulating and Experimenting proposed technique on sample images.

3.4 Providing experimental results.

3.5 Providing conclusion.

CHAPTER 2 SHAPE FROM SHADING

2.1 Introduction

Research in computer vision has attempted to provide the method for computer to recover 3D shape of the 2D image. Shading is important information for human being and also computer to use to determine shape of any object.

First proposed in 1970s, Shape from shading is a method to determine shape of the object by its shade in image. The traditional assumption in Shape from shading is based on Lambertian reflectance, known light source direction and local shape recovery. After first proposed, many researchers have proposed their techniques applied from the fundamental technique. In this proposal Shape from shading techniques are classified in to four approaches: minimization approach, propagation approach, local approach, and linear approach.

The four approaches are introduced in 2.2, follow by reflectance models in 2.3, and Implementation of Shape from shading in 2.4.

2.2 Four Approaches of Shape from Shading

Four approaches which are minimization, propagation, local, and linear approach are described in brief.

2.2.1 Minimization Approach

Techniques in minimization approach compute the shape of the object by minimizing energy function over an entire image and apply constrains to resolve unknowns. The constraints are as follows:

The Brightness constraint – indicates the total brightness error of the reconstructed image compared with the input image.

$$\iint (I - R)^2 dx\, dy \qquad (2\text{-}1)$$

The Smoothness constraint – ensures a smooth surface in order to stabilize the convergence to a unique solution.

$$\iint (p_x^2 + p_y^2 + q_x^2 + q_y^2)\, dx\, dy \qquad (2\text{-}2)$$

where p and q are surface gradients along the x and y directions. Another version of the smoothness term is

$$\iint (p_x^2 + q_y^2)\, dx\, dy \qquad (2\text{-}3)$$

and can also be described in terms of the surface normal $\vec{N}$:

$$\iint (\|\vec{N}_x\|^2 + \|\vec{N}_y\|^2)\, dx\, dy \qquad (2\text{-}4)$$

The Integrability constraint – ensures valid surfaces, that is $Z_{x,y} = Z_{y,x}$. It can be described by either

$$\int\int(p_x^{2} - q_y^{2})\, dx\, dy \tag{2-5}$$

or

$$\int\int((Z_x - p)^2 + (Z_y - q)^2)\, dx\, dy \tag{2-6}$$

The Intensity Gradient constrain – requires that the intensity gradient of the reconstructed image be close to the intensity gradient of the input image in both the x and y directions:

$$\int\int((R_x - I_x)^2 + (R_y - I_y)^2)\, dx\, dy \tag{2-7}$$

The Unit Normal constraint – forces the recovered surface normal to be unit vectors:

$$\int\int(\|\vec{N}_x\|^2 - 1)\, dx\, dy \tag{2-8}$$

2.2.2 Propagation Approach

Propagation approach starts from a single reference surface point or a set of surface points where the shape either is known or can be uniquely determined (such as singular points) and propagate the shape information across the whole image.

2.2.3 Local Approach

Local approach derives the shape by assuming local surface type. They use the intensity derivative information and assume spherical surface.

2.2.4 Linear Approach

Linear approach reduces the nonlinear problem into a linear through the linearization of the reflectance map. The idea is based on the assumption that the lower order components in the reflectance map dominate. Therefore, these algorithms only work well under this assumption.

2.3 Reflectance Model

The reflectance models can be categorized depending on their physical properties. There are Lambertian surface model, specular surface models, hybrid surface models, and more sophisticated surface models.
Some models are presented in the following.

2.3.1 Lambertian Reflectance Model

Lambertian surfaces light in all directions as diffuse reflectance. The brightness of a Lambertian surface depends on energy of the light, which fall on the surface. The amount of light energy falling on a surface element is proportional to the area of the surface element on the direction of light. The foreshortened area mentioned and can be represented as a dot product between surface normal and light source direction or a cosine of the angle between surface normal and light source where surface normal and light source direction are unit vector.

The formulae used to model Lambertian surface are:

$$I_L = R = A\rho \cos\theta_i \tag{2-9}$$

or

$$I_L = A\rho \vec{N}\,\vec{S} \tag{2-10}$$

where I_L is the Lambertian brightness

R is the reflectance map

A is the strength of the light source

θ_i is the angle between the surface normal $\vec{N} = (n_x, n_y, n_z)$ and the source direction $\vec{S} = (s_x, s_y, s_z)$

2.3.2 Specular Reflectance Model

Specularity reflects from the surface composes of specular spike and specular lobe. Incident angle of the light source in specularity is equal to the reflected angle. The light beam in the reflected angle is specular spike. Specular lobe spreads around the direction of specular spike.

The simplest model for specular reflection represents in delta function.

$$I_S = B\delta(\theta_s - 2\theta_r) \quad (2\text{-}11)$$

where I_S is the specular brightness.

B is the strength of the specular component.

θ_s is the angle between the light source direction and the viewing direction.

θ_r is the angle between the surface normal and the viewing direction.

Another model applies the Gaussian distribution as the facet orientation function and considering the other components as constants. It can be described as:

$$I_S = Ke^{-(\alpha/m)2} \quad (2\text{-}12)$$

where K is a constant.

α is the angle between the surface normal $\vec{N}$ and the bisector H of the viewing direction and source direction.

m indicates the surface roughness.

2.3.3 Hybrid Reflectance Model

Combination of Lambertian surface model and Specular surface model are hybrid surfaces. One straightforward equation for a hybrid surface is:

$$I = (1 - \omega) I_L + \omega I_S \qquad (2\text{-}13)$$

where I is the total brightness of the surface

I_L is the Lambertian brightness

I_S is the specular brightness

ω is the weight of the specular component

Another hybrid reflectance model consists of three components: diffuse lobe, specular lobe, and specular spike. The Lambertian model was used to represent the diffuse lobe, the specular component of the Torrance-sparrow model was used to model the specular lobe, and the spike component of the Beckmann Spizzichino model was used to describe the specular spike. The resulting hybrid model is given as:

$$I = K_{dl} \cos\theta_i + K_{sl}\, e^{(\beta)2/2(\sigma)2} + K_{ss}\delta(\theta_i - \theta_r)\delta(\phi_r) \qquad (2\text{-}14)$$

where K_{dl}, K_{sl}, and K_{ss} are the strengths of the three components.

β is the angle between the surface normal of the micro-facet on a patch and the mean normal of this surface patch.

σ is its standard derivation.

(θ_i, ϕ_i) is the direction of incident light in terms of the slant and tilt in 3D.

(θ_r, ϕ_r) is the direction of reflected light.

2.3.4 More Sophisticated Reflectance Models

Because of poor approximation to the diffuse component of rough surfaces of Lambertian model, more sophisticated reflectance models were introduced.

A simplified qualitative model was derived by considering the relative significance of the various terms in the function approximation

$$I = \cos\theta_i(A + B\,Max[0, \cos(\phi_r - \phi_i)]\sin\alpha \tan\beta) \qquad (2\text{-}15)$$

where $A \approx \rho(1/\pi - 0.09(m^2/(m^2 + 0.4)))$

$B \approx \rho(0.05(m^2/(m^2 + 0.18)))$

(θ_i, ϕ_i) and (θ_r, ϕ_r) are the same as in the previous section

$\alpha = Max[\theta_i, \theta_r]$

$\beta = Min[\theta_i, \theta_r]$

ρ is the albedo value

m is the surface roughness

This model is the same as Lambertian model when $m = 0$.

Clark applied perspective projection in modeling reflectance rather than orthographic projection. His model does not require light source to be at infinity. The reflectance model is

$$I(\vec{x}) = K(R(\vec{S})/(|\vec{Z}\chi + \vec{t}\,|^2/|\vec{Z}\chi|^2)) \qquad (2\text{-}16)$$

where $\vec{x} = (x,y)$ is the image coordinate vector

K is the constant

R is the reflectance map

$\vec{S} = (\vec{Z}\chi + \vec{t})/|\vec{Z}\chi + \vec{t}|$ the direction from the surface point to the light source

$\vec{t}$ is the location of the light source with respect to the coordinate system centered on the focal point of the camera

$\vec{X} = (x/f, y/f, -1)^T$, f is the focal length of the camera

Z is the depth

Hougen and Ahuja approximated the light source distribution by a set of m distinct light source vectors, $\vec{S}_1, \vec{S}_2, \ldots, \vec{S}_m$ where $\vec{S}_k$ is the average value of $\vec{S}$ over a neighborhood angle of $\vec{S}_k$. By writing $\vec{S}_k$ as a product of its magnitude λ_k and unit direction $\vec{S}_k'$, the brightness equation can be expressed by

$$I = \rho(\lambda_0 R_0 + \sum_{k=1}^{m} \lambda_k R(\vec{N}, \vec{S}_k')) \qquad (2\text{-}17)$$

where $\rho\lambda_0 R_0$ is due to the contribution of ambient light

R is the reflectance map and is dependent of the magnitude of the light source

Langer and Zucker introduced the concept of "Shape from Shading on a Cloudy Day", claimed that under diffuse lighting, the radiance depends primarily on the amount of the diffuse source visible from each surface element, with the surface normal of secondary importance and assumed the effect of mutual illumination can be ignored, the brightness at image point $\vec{x} = (x,y)$ is described as

$$I(\vec{x}) = \rho I_D \frac{1}{\pi} \int_{\upsilon(\vec{x})} \vec{N}(\vec{x}) . \vec{S} \, d\Omega \qquad (2\text{-}18)$$

where ρ is the albedo

I_D is the illuminance from the uniform hemispheric light source

$\upsilon(\vec{x})$ is the set of unit directions in which sky is visible from $\vec{x}$

$d\Omega$ is an infinitesimal solid angle

This reflectance models attempt to remove one or more of the following constraints in the Lambertian model

- The brightness is independent of the viewing direction.
- The illumination is from an infinite point source.
- The projection of the object onto the image plane is perspective.

2.4 Some Algorithms of Shape from Shading

Algorithm and implementation detail in brief are presented. The algorithms chosen are global minimization approach of Q. Zheng, and R.

Chellappa, propagation approach of M. J. Brooks, W. Chojnacki, A. van den Hengel, and W. N. Agutter and local approach of P. Tsai and M. Shah.

2.4.1 Zheng and Chellappa: Minimization Approach

Some minimization approaches apply smoothness constraint to stabilize the minimization process by convergence of the iteration process and also push the reconstruction toward a smooth surface. But smoothness constraint has several drawbacks. First, it causes the solution "to walk away" from the ground truth, even if the ground truth is used as an initial condition. Second, it flattens the reconstruction causing distortions along image discontinuities. Third, the result will depend on the value of coefficient multiply to smoothness term. Zheng and Chellappa adapt an intensity gradient constraint instead of a smoothness constraint combine with another two constraints, which are intensity constraint and integrability constraint.

Taylor series are applied to simplify reflectance map and represent the depth, gradient and their derivatives in discrete form. Then an iterative scheme is applied to update depth and gradients. The algorithm was implemented using a hierarchical structure (pyramid) in order to speed up the computation. Boundary has not to initialize specially. The initial values of both depth and gradient can be zero.

2.4.1.1 An Algorithm

From irradiance equation

$$R(p,q) = I(x,y) \tag{2-19}$$

Adaptive smoothing can be implemented by requiring the gradients of the reconstructed intensity to be equal to gradient of the input image.

$$R_x(p,q) = I_x(x,y) \tag{2-20}$$

$$R_y(p,q) = I_y(x,y) \tag{2-21}$$

Computation by interpolating, constraints are applied to form the formula.

$$\begin{aligned}&\iint (R(p,q) - I(x,y))^2 \\ &\quad + (R_p(p,q)p_x + R_q(p,q)q_x - I_x(x,y))^2 + (R_p(p,q)p_y + R_q(p,q)q_y - I_y(x,y))^2 \\ &\quad + \mu((p - Z)^2 + (q - Z)^2)\, dx\, dy\end{aligned} \tag{2-22}$$

where the first term is intensity constraint.

the second and the third term are adaptive constraints.

the fourth term is integrability constraint.

μ is a weighing factor.

Minimization is equivalent to solving the following Euler equations:

$$F_p - \frac{\partial}{\partial x} F_{px} - \frac{\partial}{\partial y} F_{py} = 0 \tag{2-23}$$

$$F_q - \frac{\partial}{\partial x} F_{qx} - \frac{\partial}{\partial y} F_{qy} = 0 \qquad (2\text{-}24)$$

$$F_Z - \frac{\partial}{\partial x} F_{Zx} - \frac{\partial}{\partial y} F_{Zy} = 0 \qquad (2\text{-}25)$$

Approximating the reflectance map around *(p,q)* by Taylor series expansion of up to first-order terms, F_p can be written as.

$$\frac{1}{2} F_p = (R - I(x,y))R + \mu(p - Z_x) \qquad (2\text{-}26)$$

Let variables with primes (') represent the values after updating variables without primes represent the values before updating.

Then

$$p' = p + \delta p, \quad q' = q + \delta q, \quad Z' = Z + \delta Z \qquad (2\text{-}27)$$

The corresponding increments in the partial derivatives of *(p,q,Z)* after updating are

$$\begin{array}{llll} p_x' = p_x + \delta p, & q_x' = q_x + \delta q, & Z_x' = Z_x + \delta Z & \\ p_y' = p_y + \delta p, & q_y' = q_y + \delta q, & Z_y' = Z_y + \delta Z & \\ p_{xx}' = p_{xx} - 2\delta p, & q_{xx}' = q_{xx} - 2\delta q, & Z_{xx}' = Z_{xx} - 2\delta Z & \\ p_{yy}' = p_{yy} - 2\delta p, & q_y' = q_{yy} - 2\delta q, & Z_{yy}' = Z_{yy} - 2\delta Z & (2\text{-}28) \end{array}$$

Substituting (39) and (40) into (38) and expanding the reflectance map R up to linear terms we obtain

$$\frac{1}{2}\ F_p = (R + R_p\delta p + R_q\delta q - I(x,y))\ R_p + \ \mu(p - Z_x + \delta p + \delta Z\ ) \quad (2\text{-}29)$$

The other terms in (2-25) can be derived and the results are list as follows:

$$\frac{1}{2}\ \frac{\partial}{\partial x}\ F_{px} = (R_p p_{xx} + R_q q_{xx} - I_{xx})R_p - 2R_p^{\ 2}\delta p - 2R_pR_q\delta q \qquad (2\text{-}30)$$

$$\frac{1}{2}\ \frac{\partial}{\partial y}\ F_{py} = (R_p p_{yy} + R_q q_{yy} - I_{yy})R_p - 2R_p^{\ 2}\delta p - 2R_pR_q\delta q \qquad (2\text{-}31)$$

$$\frac{1}{2}F_q = (R + R_p\delta p + R_q\delta q - I(x,y))R_q + \mu(q - Z_y + \delta q + \delta Z) \quad (2\text{-}32)$$

$$\frac{1}{2}\ \frac{\partial}{\partial x}\ F_{qx} = (R_p p_{xx} + R_q q_{xx} - I_{xx})R_p - 2R_pR_q\delta p - 2R_q^{\ 2}\delta q \qquad (2\text{-}33)$$

$$\frac{1}{2}\ \frac{\partial}{\partial y}\ F_{qy} = (R_p p_{yy} + R_q q_{yy} - I_{yy})R_q - 2R_pR_q\delta p - 2R_q^{\ 2}\delta q \qquad (2\text{-}34)$$

$$F_Z = 0 \qquad (2\text{-}35)$$

$$\frac{1}{2}\ \frac{\partial}{\partial x}\ F_{Zx} = -\mu(p_x - Z_{xx} - \delta p + 2\delta Z) \qquad (2\text{-}36)$$

$$\frac{1}{2}\ \frac{\partial}{\partial y}\ F_{Zy} = -\mu(q_y - Z_{yy} - \delta p + 2\delta Z) \qquad (2\text{-}37)$$

Substituting (2-39)-(2-37) into (2-25), the result can be solved.

2.4.1.2 Implementation Details

1) Hierarchical Structure: is an efficient way of reducing the computations arising in complex image-related tasks. An important advantage of

hierarchical implementation is the communication of the results from one layer to another. The input images for various resolution layers are derived from the given highest resolution image by averaging the pixels that belong to the same cell in the low-resolution layer. The surfaces shape descriptions should be consistent between different resolution layers.

- (′) stand for the shape descriptors of the higher resolution layer.
- without (′) stand for the shape descriptors of the lower resolution layer.

Rule 1: The illuminant direction and albedo are the same.

$$(\tau', \gamma', \eta', \sigma') = (\tau, \gamma, \eta, \sigma) \quad (2\text{-}38)$$

which mean they are insensitive to changes in resolution.

Rule 2: The surface descriptions of a higher resolution layer are interpolated from the descriptions of the adjacent lower resolution layer.

Let M' be the image size of the higher resolution layer.

For $i,j \in \{2, \ldots, M'\}$, the shape descriptions for the higher resolution layer are

$$(p', q', Z')_{i,j} = (p, q, 2Z)_{i/2, j/2} \quad \text{if } i \text{ and } j \text{ are evens.} \quad (2\text{-}39)$$

$$= \tfrac{1}{2}\left((p,q,2Z)_{(i+1)/2, j/2} + (p,q,2Z)_{(i-1)/2, j/2}\right) \text{ if } i \text{ is odd and } j \text{ is even.}$$

(2-40)

$$= \tfrac{1}{2}\left((p,q,2Z)_{i/2,(j+1)/2} + (p,q,2Z)_{i/2,(j-1)/2}\right) \text{ if } i \text{ is even and } j \text{ is odd.}$$

(2-41)

$$= \tfrac{1}{4}\left((p,q,2Z)_{(i+1)/2,(j+1)/2} + (p,q,2Z)_{(i+1)/2,(j-1)/2} + (p,q,2Z)_{(i-1)/2,(j+1)/2} + (p,q,2Z)_{(i-1)/2,(j-1)/2}\right) \text{ if } i \text{ and } j \text{ are odds.}$$

(2-42)

<u>Rule_3</u>: The natural boundary condition is used for the interpolation of boundary pixels.

For the boundaries of i = 1 and j = 1

$$(p',q')_{1,j} = 2(p',q')_{2,j} - (p',q')_{3,j} \qquad Z_{1,j}' = Z_{2,j}' - p_{1,j}' \qquad \text{for } j \geq 2$$

$$(p',q')_{i,1} = 2(p',q')_{i,2} - (p',q')_{i,3} \qquad Z_{i,1}' = Z_{i,2}' - q_{i,1}' \qquad \text{for } j \geq 2$$

$$(p',q')_{1,1} = 2(p',q')_{2,2} - (p',q')_{3,3} \qquad Z_{1,1}' = Z_{2,2}' - p_{1,1}' - q_{1,1}' \qquad (2\text{-}43)$$

1) Iterative scheme:

<u>Step_1</u> Estimation of the reflectance map parameters (τ, γ, η, σ)

<u>Step_2</u> Normalization of the input image:

$$I' = (I - \sigma)/\eta \qquad (2\text{-}44)$$

Reduce the input image size to that of the lowest resolution layer and set the values of p^0, q^0 and Z^0 to zero.

Step_3 Update the current shape reconstruction. For each pixel, the partial derivatives are approximated by

$$p_x = p^k_{(x+1,y)} + p^k_{(x,y)} \quad (2\text{-}45)$$

$$p_{xx} = p^k_{(x+1,y)} + p^k_{(x-1,y)} - 2\,p^k_{(x,y)} \quad (2\text{-}46)$$

$$p_{yy} = p^k_{(x,y+1)} + p^k_{(x,y-1)} - 2\,p^k_{(x,y)} \quad (2\text{-}47)$$

$$q_y = q^k_{(x,y+1)} + q^k_{(x,y+1)} \quad (2\text{-}48)$$

$$q_{xx} = q^k_{(x+1,y)} + q^k_{(x-1,y)} - 2q^k_{(x,y)} \quad (2\text{-}49)$$

$$q_{yy} = q^k_{(x,y+1)} + q^k_{(x,y-1)} - 2q^k_{(x,y)} \quad (2\text{-}50)$$

$$Z_x = Z^k_{(x+1,y)} - Z^k_{(x,y)} \quad (2\text{-}51)$$

$$Z_{xx} = Z^k_{(x+1,y)} - Z^k_{(x-1,y)} - 2Z^k_{(x,y)} \quad (2\text{-}52)$$

$$Z_y = Z^k_{(x,y+1)} - Z^k_{(x,y)} \quad (2\text{-}53)$$

$$Z_{yy} = Z^k_{(x,y+1)} - Z^k_{(x,y-1)} - 2Z^k_{(x,y)} \quad (2\text{-}54)$$

$$I'_{xx} = I'_{(x+1,y)} + I'_{(x-1,y)} - 2I'_{(x,y)} \quad (2\text{-}55)$$

$$I'_{yy} = I'_{(x,y+1)} + I'_{(x,y-1)} - 2I'_{(x,y)} \quad (2\text{-}56)$$

where we use natural boundary conditions similar to Rule 3 for values outside the image frame. The shape reconstruction is updated by:

$$\delta p = (C_1A_{22} - C_2A_{12})/\Delta \qquad p^{k+1} = p^k + \delta p \quad (2\text{-}57)$$

$$\delta q = (C_2A_{11} - C_1A_{12})/\Delta \qquad q^{k+1} = q^k + \delta q \quad (2\text{-}58)$$

$$\delta Z = (C_3 - \delta p + \delta q)/4 \qquad Z^{k+1} = Z^k + \delta Z \quad (2\text{-}59)$$

where

$$A_{11} = 5R_p^2 + 1.25\mu \quad (2\text{-}60)$$

$$A_{12} = 5R_pR_q + 0.25\mu \quad (2\text{-}61)$$

$$A_{22} = 5R_q^2 + 1.25\mu \qquad (2\text{-}62)$$

$$R = R(p^k_{(x,y)},\ q^k_{(x,y)}) \qquad (2\text{-}63)$$

$$R = R_p(p^k_{(x,y)},\ q^k_{(x,y)}) \qquad (2\text{-}64)$$

$$R = R_q(p^k_{(x,y)},\ q^k_{(x,y)}) \qquad (2\text{-}65)$$

$$C_3 = -p_x - q_y + Z_{xx} + Z_{yy} \qquad (2\text{-}66)$$

$$C_1 = (\varepsilon\text{-}\varepsilon)R_p - \mu(p^k - Z_x) - 0.25\mu C_3 \qquad (2\text{-}67)$$

$$C_2 = (\varepsilon\text{-}\varepsilon)R_q - \mu(q^k - Z_y) - 0.25\mu C_3 \qquad (2\text{-}68)$$

$$\varepsilon = R - I'_{(x,y)} \qquad (2\text{-}69)$$

$$\varepsilon = R(p_{xx} + p_{yy}) + R(q_{xx} + q_{yy}) - I'_{xx} - I'_{yy} \qquad (2\text{-}70)$$

$$\Delta = A_{11}A_{22} - A_{12}^2 \qquad (2\text{-}71)$$

If {(Solution is stable) OR (Iteration has reached N_{max} of current layer)}

continue to Step 4

else

repeat Step 3

endif.

<u>Step_4</u>

If {Current image is in the highest resolution}

stop

else

- Increase the image size and expand the shape reconstruction to the adjacent higher resolution layer by (51)-(52).
- Reduce the normalized input image to the current resolution.
- Go to Step 3.

endif

2.4.2 Tsai and Shah: Linear Approach

This is a simple algorithm of Ping-Sing Tsai and Mubarak Shah, which is a linear approach. Tsai and Shah applied discrete approximation of the gradient and then employed linear approximation of the reflectance function in terms of the depth. Both Lambertian surface model and Specular surface model are introduced in his paper. Lambertian surface model is chosen to represent along with implementation details.

2.4.2.1 An Algorithm

The reflectance function for the Lambertian surface model is

$$E(x,y) = R(p,q) \tag{2-72}$$

$$= \frac{1 + pp_s + qq_s}{(1+p^2+q^2)^{1/2}(1+p_s^2+q_s^2)^{1/2}} \tag{2-73}$$

$$= \frac{\cos\sigma + p\cos\tau\sin\sigma + q\sin\tau\cos\sigma}{(1+p^2+q^2)^{1/2}} \tag{2-74}$$

where $E(x,y)$ is gray level at pixel (x,y),

$p = \frac{\partial Z}{\partial x}$ and, $q = \frac{\partial Z}{\partial y}$, are gradient of surface normal

$p_s = \dfrac{\cos\tau\sin\sigma}{\cos\sigma}$ and, $q_s = \dfrac{\sin\tau\sin\sigma}{\cos\sigma}$, are gradient of light source

τ is the tilt of the illuminant.

σ is the slant of the illuminant.

Then apply discrete approximations for p and q

$$p = \frac{\partial Z}{\partial x} = Z(x,y) - Z(x\text{-}1,y) \tag{2-75}$$

$$q = \frac{\partial Z}{\partial y} = Z(x,y) - Z(x,y\text{-}1) \tag{2-76}$$

Rewritten the reflectance equation as:

$$0 = f(E(x,y), Z(x,y), Z(x\text{-}1,y), Z(x,y\text{-}1)) \tag{2-77}$$

$$= E(x,y) - R(Z(x,y) - Z(x\text{-}1,y),\ Z(x,y) - Z(x,y\text{-}1)) \tag{2-78}$$

Linear approximation (Taylor series expansion up through the first order terms) of the function f about a given depth map Z^{n-1} is

$$0 = f(E(x,y), Z(x,y), Z(x\text{-}1,y), Z(x,y\text{-}1)) \tag{2-79}$$

$$\approx f(E(x,y), Z^{n-1}(x,y), Z^{n-1}(x\text{-}1,y), Z^{n-1}(x,y\text{-}1))$$

$$+ (Z(x,y) - Z^{n-1}(x,y))\ \frac{\partial}{\partial Z(x,y)} f(E(x,y),\ Z^{n-1}(x,y),\ Z^{n-1}(x\text{-}1,y),\ Z^{n-1}(x,y\text{-}1))$$

$$+ (Z(x\text{-}1,y) - Z^{n-1}(x\text{-}1,y))\ \frac{\partial}{\partial Z(x-1,y)} f(E(x,y),\ Z^{n-1}(x,y),\ Z^{n-1}(x\text{-}1,y),\ Z^{n-1}(x,y\text{-}1))$$

$$+ (Z(x,y-1) - Z^{n-1}(x,y-1)) \frac{\partial}{\partial Z(x,y-1)} f(E(x,y), Z^{n-1}(x,y), Z^{n-1}(x-1,y), Z^{n-1}(x,y-1))$$

(2-80)

Then Z and Z^{n-1} are separated on each side of equation.

$$\frac{\partial}{\partial Z(x,y-1)} f(E(x,y), Z^{n-1}(x,y), Z^{n-1}(x-1,y), Z^{n-1}(x,y-1)) * Z(x,y-1)$$

$$+ \frac{\partial}{\partial Z(x-1,y)} f(E(x,y), Z^{n-1}(x,y), Z^{n-1}(x-1,y), Z^{n-1}(x,y-1)) * Z(x-1,y)$$

$$+ \frac{\partial}{\partial Z(x,y)} f(E(x,y), Z^{n-1}(x,y), Z^{n-1}(x-1,y), Z^{n-1}(x,y-1)) * Z(x,y)$$

$$= - f(E(x,y), Z^{n-1}(x,y), Z^{n-1}(x-1,y), Z^{n-1}(x,y-1))$$

$$+ Z^{n-1}(x,y) * \frac{\partial}{\partial Z(x,y)} f(E(x,y), Z^{n-1}(x,y), Z^{n-1}(x-1,y), Z^{n-1}(x,y-1))$$

$$+ Z^{n-1}(x-1,y) * \frac{\partial}{\partial Z(x-1,y)} f(E(x,y), Z^{n-1}(x,y), Z^{n-1}(x-1,y), Z^{n-1}(x,y-1))$$

$$+ Z^{n-1}(x,y-1) * \frac{\partial}{\partial Z(x,y-1)} f(E(x,y), Z^{n-1}(x,y), Z^{n-1}(x-1,y), Z^{n-1}(x,y-1))$$

(2-81)

The depth value $Z(x,y)$ at the n^{th} iteration can be solved using the previous estimates, $Z^{n-1}(i,j)$, for all the $Z^{n-1}(i,j)$ with $i \neq x$ and $j \neq y$. Substitute $Z(x-1,y)$ and $Z(x,y-1)$ with $Z^{n-1}(x-1,y)$ and $Z^{n-1}(x,y-1)$ in equation (32) then the third and fourth terms on the right hand side cancelled out. The equation reduces in the following.

$$0 = f(Z(x,y)) \qquad (2\text{-}82)$$

$$\approx f(Z^{n-1}(x,y)) + (Z(x,y) - Z^{n-1}(x,y))\frac{d}{dZ(x,y)} f(Z^{n-1}(x,y)) \qquad (2\text{-}83)$$

Then for $Z(x,y) = Z^n(x,y)$, depth map at the n-th iteration can be solved.

$$Z^n(x,y) = Z^{n-1}(x,y) + (-f(Z^{n-1}(x,y)))/ \left(\frac{d\, f(Z^{n-1}(x,y))}{dZ(x,y)}\right) \qquad (2\text{-}84)$$

where

$$\frac{d\, f(Z^{n-1}(x,y))}{dZ(x,y)} = 1*\left(\frac{(p_s + q_s)}{(p^2+q^2+1)^{1/2}(p_s^2+q_s^2+1)^{1/2}}\right)-$$

$$\left(\frac{(p+q)(pp_s+qq_s+1)}{(p^2+q^2+1)^{3/2}(p_s^2+q_s^2+1)^{1/2}}\right) \qquad (2\text{-}85)$$

Assume the initial estimate of $Z^0(x,y) = 0$ for all pixels, the depth map can be iteratively refined using equation (2-83).

2.4.2.2 Implementation Details

Assuming the initial estimate of $Z^0(x,y) = 0$ for all pixel.

Equation (2-83) is refined for the depth map. Iterative computation of the function $f(Z^{n-1}(x,y))$, and the first derivative of the function $f'(Z^{n-1}(x,y))$ are needed. Notice that $f'(Z^{n-1}(x,y))$ cannot be zero since that cause the division by zero. So equation (2-83) is rewritten as follows:

$$Z^n(x,y) = Z^{n-1}(x,y) + K^n(-f(Z^{n-1}(x,y))) \qquad (2\text{-}86)$$

where K^n needs to satisfy three constraints:

1. K^n is approximately equal to the inverse of $\dfrac{df(Z^{n-1}(x,y))}{dZ(x,y)}$

2. K^n equals zero when $\dfrac{df(Z^{n-1}(x,y))}{dZ(x,y)}$ approaches zero.

3. K^n becomes zero when $Z^n(x,y)$ approaches to true $Z(x,y)$

K^n is defined as follows:

$$K^n = \frac{S^n_{x,y} M_{x,y}}{W_{x,y} + S^n_{x,y} M_{x,y}} \qquad (2\text{-}87)$$

where $M_{x,y} = \dfrac{df(Z^{n-1}(x,y))}{dZ(x,y)}$

$S_{x,y}{}^n = E[(Z^n(x,y) - Z(x,y))^2]$

E is the expectation operator.

$W_{x,y}$ is small, but non-zero.

$$\text{Then} \quad K^n \approx \frac{1}{M_{x,y}} \qquad (2\text{-}88)$$

So $\quad K^n$ is the inverse of $\dfrac{df(Z^{n-1}(x,y))}{dZ(x,y)}$

$M_{x,y}$ approaches to zero, K^n becomes zero.

$S_{x,y}{}^n$ becomes zero, when $Z^n(x,y)$ approach to true $Z(x,y)$

Clearly that definition of K^n satisfies all three constraints.

CHAPTER 3 OPTIMAL THRESHOLDING

3.1 Introduction to Thresholding

Thresholding is a method in image processing to extract some parts of an object or some objects from a gray-scale image. Considering a histogram, gray-scale image can determine the contents such as number of objects by counting groups of the gray level in the histogram. Thresholding use gray level as a mean to find threshold to extract the objects from one another.

Suppose that a gray-level histogram corresponds to an image $f(x,y)$, which composed of light objects on a dark background. The histogram illustrates gray level grouped into two dominant modes. To extract the objects from the background is to find the threshold T which for any point (x,y)

$$O = \{f(x,y) \mid f(x,y) > T\} \tag{3-1}$$

$$B = \{f(x,y) \mid f(x,y) \leq T\} \tag{3-2}$$

where O is the set of objects.

B is the set of background.

Extracting more than one object from one another, more than one threshold is required, and called *mutilevel thresholding.*

For function T, define $p(x,y)$ is the local property of point (x,y), and $f(x,y)$ is the gray level of point (x,y). If T depends only on $f(x,y)$ the threshold is called *global.* If T depends on both $f(x,y)$ and $p(x,y)$ the threshold is called *local.* Finally, if T depend on spatial coordinates x and y the threshold is called *dynamic.*

3.2 Optimal Thresholding

Optimal Thresholding is introduced base on the assumption that the image determined contains two principal brightness regions. Thresholding processes start by dividing parts of image into brighter and darker region. For the image with more than two brightness regions, the division can further process each region into two more regions. The processes terminate when the image has satisfying segmented parts.

Suppose that an image contains two values combined with additive Gaussian noise. The mixture probability density function is

$$p(z) = P_1 p_1(z) + P_2 p_2(z) \qquad (3\text{-}3)$$

where $p(z)$ is brightness probability density function

$$p(z) = P_1/(\sigma_1(2\pi)^{1/2})\ exp[-(z-\mu_1)^2/(2\sigma_1^2)] + P_2/(\sigma_2(2\pi)^{1/2})\ exp[-(z-\mu_2)^2/(2\sigma_2^2)] \qquad (3\text{-}4)$$

where μ_1 and μ_2 are the mean values of the two brightness levels.

σ_1 and σ_2 are the standard deviations about the means.

P_1 and P_2 are a priori probabilities of the two levels.

The constraint that must be satisfied is

$$P_1 + P_2 = 1 \tag{3-5}$$

Assume the object as the brighter region, $\mu_1 < \mu_2$, the probability of classifying and object point as a background point is

$$E_1(T) = \int_{-\infty}^{T} p_2(z)dz \tag{3-6}$$

and the probability of classifying a background point as an object point is

$$E_2(T) = \int_{-\infty}^{T} p_1(z)dz \tag{3-7}$$

Then the overall probability of error is

$$E(T) = P_2\, E_1(T) + P_1\, E_2(T) \tag{3-8}$$

To get the minimum error, differentiate $E(T)$ with respect to T and set the result to 0.

$$P_1\, p_1(T) = P_2 p_2(T) \tag{3-9}$$

Apply the result to Gaussian density, take logarithms, and simplify, give quadratic equation

$$AT^2 + BT + C = 0 \tag{3-10}$$

where

$$A = \sigma_1^2 - \sigma_2^2 \quad (3\text{-}11)$$

$$B = 2(\mu_1\sigma_2^2 - \mu_2\sigma_1^2) \quad (3\text{-}12)$$

$$C = \sigma_1^2\mu_2^2 - \sigma_2^2\mu_1^2 + 2\sigma_1^2\sigma_2^2 ln((\sigma_2 P_1)/(\sigma_1 P_2)) \quad (3\text{-}13)$$

The two values can be gained by solving the quadratic equation then choose a reasonable value be a threshold.

3.3 Implementation of Optimal Thresholding

The two results of quadratic function are:

$$T_1 = (-B + (B^2 - 4AC)^{1/2})/2A \quad (3\text{-}14)$$

$$T_2 = (-B - (B^2 - 4AC)^{1/2})/2A \quad (3\text{-}15)$$

Assuming the priori probabilities to be equal.

$$P_1 = P_2 = 0.5 \quad (3\text{-}16)$$

The other initial values can be obtained by dividing the histogram into two parts about its mean value. The mean of each part then been computed by.

$$\mu = \frac{\left(\sum_N x\right)}{N} \quad (3\text{-}17)$$

where x is value of gray level of each pixel in the image presenting on the histogram of that part.

N is number of pixel in the image presenting on that part of the histogram.

The standard deviation of each part is

$$\sigma = \left(\sum_{N} \frac{(x-\mu)^2}{N} \right)^{1/2} \quad (3\text{-}18)$$

where μ is the mean of that part of the histogram.

The priori probability can be determined from

$$P = \frac{\sum_{N} x}{\sum_{M} x} \quad (3\text{-}19)$$

where M is the total number of pixel of the image presented of the whole histogram.

Find the threshold by

$$T^{(m+1)} = (\mu_0^{(m)} + \mu_1^{(m)})/2 \quad (3\text{-}20)$$

The process performed iteratively find threshold T and terminate when $T^{(m+1)} = T^{(m)}$ at the $(m+1)$-th iteration.

CHAPTER 4 HISTOGRAM PROCESSING

4.1 Introduction

Histogram of gray level image is a graph to represent gray level of the image versus the number of pixels in each level which can present the characteristics of the image in global view. In digital image processing, histogram processing is the process to manipulate histogram of an image to affect the gray level of the image. For the image with gray level of range [0, L-1] its histogram is a bar of discrete function

$$p(r_k) = n_k/N \qquad (4\text{-}1)$$

where r_k is the k th gray level

n_k is the number of pixel in the k th level

N is the number of pixel in the image

By histogram processing, information of the image can be manipulated and enhanced. In this chapter Histogram Equalization and Histogram Specification will be presented in 4.2 and 4.3 respectively.

4.2 Histogram Equalization

Histogram Equalization is the way to enhance the contrast of the image by the global intensity distribution. The technique reflects the idea of flattening out the histogram, or making the histogram closest to the probability density function of the uniform distribution and lets the spacing between gray levels be proportional to the frequency of that gray level.

4.2.1 Implementation Details

1. Find probability density function of gray level of the image.

$$p_r(r_k) = n_k/N \qquad (4\text{-}2)$$

where k is in the interval $[0, L\text{-}1]$

r_k is in the interval $[0, 1]$

n_k is number of pixels in k level

N is the total number of pixel in the image.

2. Find transformation function s_k by

$$s_k = T(r_k) = \sum_{j=0}^{k} \frac{n_j}{N} = \sum_{j=0}^{k} p_r(r_j) \qquad (4\text{-}3)$$

3. For every value k in the image replace k with round down of the multiplication of s_k and $L\text{-}1$

$$I(m,n) = round(s_k * (L\text{-}1)) \qquad (4\text{-}4)$$

where $I(m,n)$ is the intensity value of k of the pixel (m,n) in the image

4.3 Histogram Specification

Histogram Specification is similar to Histogram Equalization which both can be applied to improve contrast of image. Instead of making the output histogram uniform, Histogram Specification can be applied to make it whatever is wanted. That is output histogram can be specified in shape.

4.3.1 Implementation Details

1. Find transformation function s_k or $T(r_k)$of the original image by applying step 1 and 2 of Histogram Equalization.
2. Find transformation function v_k or $G(z_k)$ of the desired histogram by repeating step 1 and 2 of the
3. For every value k in the image replace k with round down of the multiplication of $G(s_k(k)(L-1))$ and $L-1$

$$I(m,n) = round(G(s_k(k)*(L-1))*(L-1)) \quad (4\text{-}5)$$

where $I(m,n)$ is the intensity value of k of the pixel (m,n) in the image

CHAPTER 5 PROPOSED TECHNIQUES

5.1 Introduction

The proposed techniques used to prepare the 2D image by applied processes of Optimum Thresholding and Histogram Processing which are Histogram Equalization by Zones for 2 Zones (HEQBZ_2Z), Histogram Specification by Zones for 2 Zones (HSPBZ_2Z), Histogram Equalization by Zones for Multiple Zones (HEQBZ_MZ) and Histogram Specification by Zones for Multiple Zones (HSPBZ_MZ).

5.2 Concept of the Proposed Techniques

Since the image which is low contrast or too dark (low intensity) or ambiguity 2D image resulting in ambiguity in generated 3D. The proposed techniques are tried to present enhance in contrast of the 2D image reasonably. Optimal Thresholding is applied to divide histogram of the image in zone for distributing intensity of the image thoroughly by Histogram Equalization and Histogram Specification.

5.3 HEQBZ_2Z

HEQBZ_2Z performs by first dividing histogram of the image into 2 zones and then apply histogram equalization to each zone.

5.3.1 Implementation Details

1. Find histogram of the original image.
2. From histogram of the original image, applied Optimal Thresholding to the histogram to get a threshold.
3. Find the probability density function p_k of the image.

$$p(k) = n_k/N \tag{5-1}$$

where k is in the interval $[0, L-1]$

n_k is number of pixels in k level of histogram

N is the total number of pixel in the image.

4. Divide histogram of the image into 2 zones by the threshold. Find the transformation function For the first zone

$$s_{k1} = round\left(\left(\sum_{k=0}^{T} p(k)\right) * (L-1)\right) \tag{5-2}$$

For the other zone

$$s_{k2} = round\left(\left(\sum_{k=T+1}^{L-1} p(k)\right) * (L-1)\right) \tag{5-3}$$

where k is the level of the gray level

T is the threshold

$p(k)$ is probability density of the gray level at level k

L is the number of levels of histogram

5. Substitute all pixel in the image by

the first zone,

$$I(i,j) = s_{k1} \tag{5-4}$$

the last zone, round down of multiplication of s_k and L plus T

$$I(i,j) = T + s_{k2} \tag{5-5}$$

where I(i,j) is the gray value of the pixel *(i,j)*

5.4 HSPBZ_2Z

HSPBZ_2Z is Histogram Specification by zones for 2 zones which performs by combining Histogram specification using Gaussian density as a desired probability density function and Optimal Thresholding.

5.4.1 Implementation Details

1. Find histogram of the original image.
2. Find a threshold by appling Optimal Thresholding
3. Find probability density function *p(k)* like step 3 of HEQBZ_2Z
4. Find s_k of the histogram by for any k summation of all *p(k-1)* to *p(0)* multiply with *L-1* and round down the result.

$$s_k = round\left(\left(\sum_{k=0}^{L-1} p(k)\right) * (L-1)\right) \tag{5-6}$$

5. Divide histogram into 2 zones by the threshold and then find means and standard deviations of each zone.

For the first zone, mean is calculated by

$$\mu_1 = \frac{\left(\sum_{z=0}^{T} x_z\right)}{N} \tag{5-7}$$

where μ_1 is the mean of the first zone

z is the gray level of the histogram

x_z is number of pixels of the gray level z

T is the threshold.

N is the number of pixels of the first zone of the histogram

and standard deviation of the first zone is

$$\sigma_1 = \left(\frac{\sum_{z=0}^{T}(x_z - \mu_1)^2}{N}\right)^{1/2} \tag{5-8}$$

where σ_1 is the standard deviation of the first zone

For the other zone, mean is calculated by

$$\mu_2 = \frac{\left(\sum_{z=T+1}^{L-1} x_z\right)}{M} \tag{5-9}$$

where μ_2 is mean of the last zone

L is number of levels of the histogram

M is number of pixels of the last zone of the histogram

and standard deviation of the last zone is

$$\sigma_2 = \left(\frac{\sum_{z=T+1}^{L-1} (x_z - \mu_2)^2}{M} \right)^{1/2} \qquad (5\text{-}10)$$

where σ_2 is standard deviation of the last zone

6. Find desired probability density function p_z by using means and standard deviation of step 5.

   For the first zone

$$p(z) = (N+M) / (\sigma_1 (2\pi)^{1/2}) \, exp[-(z-\mu_1)^2/(2\sigma_1^2)] \qquad (5\text{-}11)$$

   where z is in the interval $[0,T]$

   For the last zone

$$p(z) = (N+M) / (\sigma_2 (2\pi)^{1/2}) \, exp[-(z-\mu_2)^2/(2\sigma_2^2)] \qquad (5\text{-}12)$$

   where z is in the interval $[T+1,L-1]$

7. Find transformation function g_z by

$$g_z = round\left(\left(\sum_{z=0}^{L-1} p(z) \right) * (L-1) \right) \qquad (5\text{-}13)$$

8. Substitute every pixel with gray level k by $g_z(s_k(k))$

$$I(i,j) = g_z(s_k(k)) \qquad (5\text{-}14)$$

5.5 HEQBZ_MZ

Similar to HEQBZ_2Z, HEQBZ_MZ performs by combination of Histogram equalization and Optimal Thresholding. Instead of dividing histogram into 2 zones by a threshold, HEQBZ_MZ divide histogram into more than 2 zones by more than a threshold. The number of thresholds depends on the suitability of each image.

5.5.1 Implementation Details

1. Find histogram of the image.
2. Applied Optimal Thresholding to get multiple thresholds.
3. Find the probability density function p_k of the image.
4. Find s_k of each zone similar to step 4. of HEQBZ_2Z

   For the first zone s_{k1} is calculate by the same way as HEQBZ_2Z

   $$s_{k1} = round\left(\left(\sum_{k=0}^{T_1} p(k)\right) * (L-1)\right) \tag{5-15}$$

   where $T1$ is the first threshold

   For the second zone s_{k2} is

   $$s_{k2} = round\left(\left(\sum_{k=T_1+1}^{T_2} p(k)\right) * (L-1)\right) \tag{5-16}$$

   For the n zone s_{kn} is

   $$s_{kn} = round((\left(\left(\sum_{T_{n-1}+1}^{T_n} p(k)\right) * (L-1)\right) \tag{5-17}$$

5. Like step 5 of the HEQBZ_2Z

   For the first zone

$$I(i,j) = s_{kl} \quad (5\text{-}18)$$

For the *n* zone

$$I(i,j) = Tn\text{-}1 + s_{kl} \quad (5\text{-}19)$$

5.6 HSPBZ_M

Like HSPBZ_2Z, HSPBZ_MZ performs by combination of Histogram Specification and Optimal Thresholding. Unlike HSPBZ_2Z, HSPBZ_MZ divides histogram of the image into more than 2 zones with more than one threshold.

5.6.1 Implementation Details

Like HSPBZ_2Z but the histogram will be divided into many zones.

1. Find histogram of the original image.
2. Find multiple thresholds of the histogram.
3. Find the probability density function p_k of the original histogram.
4. Find transformation function of the original image s_k
5. Find means and standard deviations of each zone.
6. From means and standard deviation, Find probability function $p(z)$ of each zone.
7. From $p(z)$, find transformation function g_z
8. Substitute $g_z(s_k(k))$ to all the pixels in the image.

CHAPTER 6 EXPERIMENTAL RESULTS

6.1 Overview of The Results

The experimental results are received from two modules: the processes in 2D image module and 3D generating module. The combination of histogram processing and Optimal Thresholding for process 2D image before passing to Shape from Shading module to produce the 3D image. The 3D results from Shape from Shading of Tsai and Shah's algorithm are linear approach with reasonable results. Six techniques are applied to be compared in result with one another for each image. There are histogram equalization, histogram specification, HEQBZ_2Z, HSPBZ_2Z, HEQBZ_MZ and HSPBZ_MZ.

For Shape from Shading due to disadvantage of the technique which determine depth of the image from intensity, parts of the image which have low intensity or darker part will be look flatter when generated into 3D whether there are flat or not in 2D. All six techniques applied to 2D images are needed to give the images more contrast to stretch their histograms to provide less ambiguity of the gray level images. Nevertheless too high in contrast will effect the quality of the results by unreasonable in relative depth of 3D.

The results of some proposed technique look better than the original images for the 2D image which have some shadows or darker parts in the image like the left side of the face in Lenna image and the right side of the face in Debbie image. For the low contrast image like Paolina and Zelda image the results are better for the 2D image after the proposed technique, which have the more in number of pixels in the lighter part of the histogram than the original image and distribute the intensity more reasonably. For bird image which is quite high in contrast and has more in number of lighter pixels than any other images when notice in the histogram, give the worse result than the original image in all six techniques. Pepper image provides comparable results in all technique when compared to the original.

6.2 Results of Original Images

3D generated from original image without any processing have smoother look among seven images (images after six techniques and original image) except for Debbie image which the other six image after processing image have better and smoother look.

6.3 Results of Images after Histogram Equalization Process

The result of uniform histogram stretching or contrast enhance of Histogram Equalization give the better image when compared to the original image in some image 3D of Pepper image has a more complete look at the branch of the paprika. 3D of Debbie image has a better look for the whole image when compare to the 3D of the original, especially for the right side of her face which cover with shadow in the original 2D.

6.4 Results of Images after Histogram Specification Process

Notice in the histograms of the image after Histogram Specification process, middle part of the histograms will have been stretched longer than the other parts. Those are because of choosing Gaussian probability density function as a desired histogram which makes the 2D images too high in contrast and finally result in 3D image generated such as Paolina image. The results from this technique are worse than the original image except for Debbie image which this technique give the best result since the histogram of the image stretched most reasonably by this technique

6.5 Results of Images after HEQBZ_2Z Process

Histogram of images after HEQBZ_2Z are divided into two zones because of the intention to give the histogram to stretch more reasonably. Results of this technique have a step look when compared to results from Histogram Equalization which give worse results in some image but give better in some image such as Lenna, pepper and Paolina.

6.6 Results of Images after HSPBZ_2Z Process

Like HEQBZ_2Z, this technique divides histogram into two parts because of the intention to stretch the histogram more reasonable but result in this step look 3D. Like Histogram Specification technique, HSPBZ_2Z give the image which higher in contrast in each zone when compare to HEQBZ_2Z. Results of HSPBZ_2Z are much like HEQBZ_2Z but better in Debbie.

6.7 Results of Images after HEQBZ_MZ Process

When dividing the histogram into more zones, results of HEQBZ_MZ are much better in Zelda and Lenna. For Lenna image, this technique gives the best result since the image after HEQBZ_MZ has a reasonable distributing in intensity the maximum number of pixel in each gray level is not greater than 900. For Paolina image result of this technique is comparable to the result of the original image since image and background of the image are separate clearly after zoning and histogram processing.

6.8 Results of Images after HSPBZ_MZ Process

3D of images after HSPBZ_MZ are comparable in every image of the Histogram Specification type of technique (Histogram Specification, HSPBZ_2Z, HEQBZ_MZ).

After 3D reconstruction, converted 2D images from 3D are generated, the results of converted 2D images are not so different from 3D. For Histogram Specification kind of techniques (Histogram Specification, HSPBZ_2Z, HSPBZ_MZ) converted 2D images look so clear but 3D are not so nice since 2D images before reconstruction process have too high contrast.

CHAPTER 7 CONCLUSION

Form experimental results we can conclude that proposed techniques can improve in generating 3D by relieving effect of darkness and ambiguity of 2D image. The conclusions are

1. From the test images, the results of histogram equalization techniques (Histogram Equalization, HEQBZ_2Z, HEQBZ_MZ,) give the better results than histogram specification techniques (Histogram Specification, HSPBZ_2Z, HSPBZ_MZ) because of the characteristics of the image which can be noticed from histogram. But for the image which has high number of pixel in the darker side the Histogram Specification technique kind will give in better result which results from choosing Gaussian distribution density function as a desired shape of histogram.

2. From the test images, in most of the results of zoning techniques (HEQBZ_2Z, HSPBZ_2Z, HEQBZ_MZ, HSPBZ_MZ) will give the more step look in 3D generated than no zoning techniques (Histogram Equalization, Histogram Specification)

BIBLIOGRAPHY

[1] Bichsel, M; and A. P. Pentland, *A Simple Algorithm for Shape from Shading*, IEEE Proc. Computer Vision and Pattern Recognition, page 459-465, 1992.

[2] Brooks, Michael J; Wojciech Chojnacki, Anton van den Hengel, and Wayne N. Agutter, *Solving the shape-from-shading problem on the CM-5*, Proc. Computer Architectures and Machine Perception, IEEE Society Press, Como, Italy, September, 1995, page196-201.

[3] Cho Siu-Yeung. and Tommy W. S. Chow, *Shape and Surface Measurement Technology by an Improved Shape-From-Shading Neural Algorithm*, IEEE Transactions on Industrial Electronics, 47 (1), February 2000,page 225-230.

[4] Dupuis, Paul. and John Oliensis, *Direct Method For Reconstructing Shape From Shading*, Computer Vision and Pattarn Recognition 92, pages 453--458, 1992.

[5] Gonzalez, Rafael C. and Richard E. Woods, *Digital Image Processing*, Addison-Wesley Publishing Company

[6] Horn, B.K.P. *Height and gradient from shading*, International Journal of Computer Vision, pages 37-75,1989.

[7] Kreyszig, Erwin; *Advanced Engineering Mathematics*, sixth edition,Wiley

[8] Leclerc, Yvan G; and Aaron F. Bobick, *The Direct Computation of Height from Shading*, IEEE Proc.Computer Vision and Pattern Recognition, page 552-558, 1991.

[9] Opimal Thresholding, download from http://ct.radiology.uiowa.edu/~jiangm/courses/dip/html/node121.html

[10] Pentland, Alex. *Shape Information From Shading: A Theory About Human Perception*, Proc. Int'l Conf. Computer Vision, page 404-413, 1988.

[11] Thresholding, download from http://ct.radiology.uiowa.edu/~jiangm/courses/dip/html/node119.html

[12] Tsai, Ping-Sing; and Mubarak Shah, *Shape from Shading Using Linear Approximation*, Technical report from the Department of Computer Science, University of Central Florida, Orlando, FL 32816.

[13] Zhang, Ruo; Ping-Sing Tsai, James Edwin Cryer, and Mubarak Shah, *Analysis of Shape from Shading Techniques*, download from ftp://eustis.cs.ucf.edu/pub/tech_paper/SFS_survey

[14] Zhang, Ruo; Ping-Sing Tsai, James Edwin Cryer, and Mubarak Shah, *Shape from Shading: A Survey*, Trans. IEEE Pattern Analysis and Machine Intelligence, August, 1999, Vol.21, No.8, page 690-760.

[15] Zhang, Ruo; Ping-Sing Tsai, James Edwin Cryer, and Mubarak Shah, *Analysis of Shape from Shading Techniques*, IEEE Computer Vision and Pattern Recognition-94, Seattle, Washington, June 20-24, pages 377-384.

[16] Zheng, Qinfen; and Rama Chellappa, *Estimation of Illuminant Direction, Albedo, and Shape from Shading*, IEEE Trans. Pattern Analysis and Machine Intelligence, Vol.13 No. 7, page 680-702, 1991.

APPENDIX A

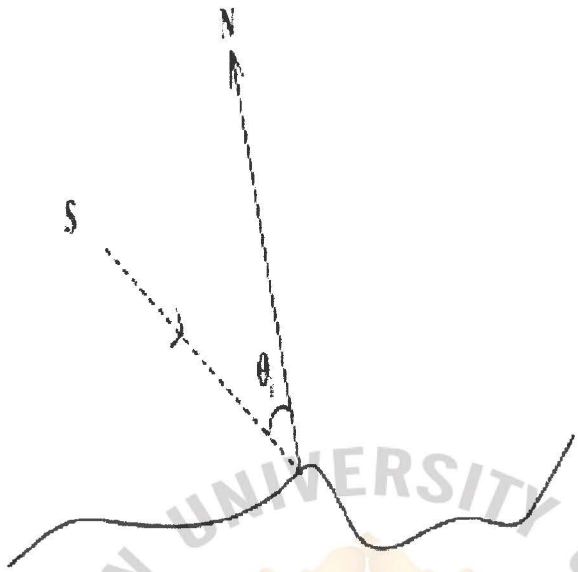

Fig.2-1 Lambertian reflection geometry

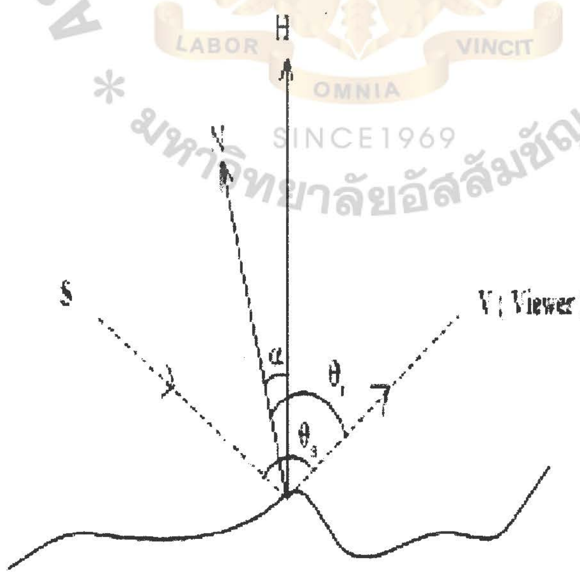

Fig.2-2 Specular reflection geometry

APPENDIX B

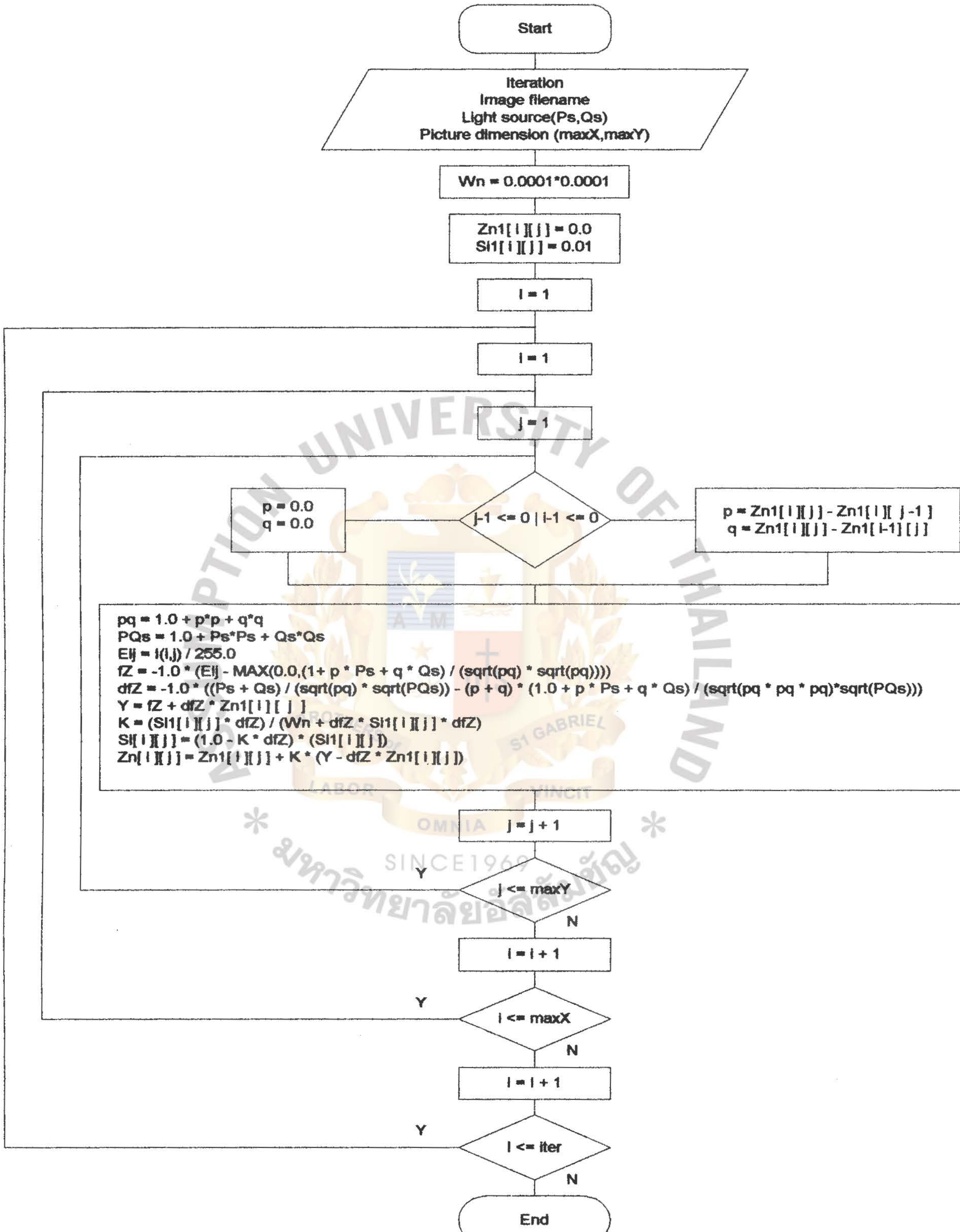

Figure 2-3 Tsai and Shah 's Algorithm Flowchart

APPENDIX C

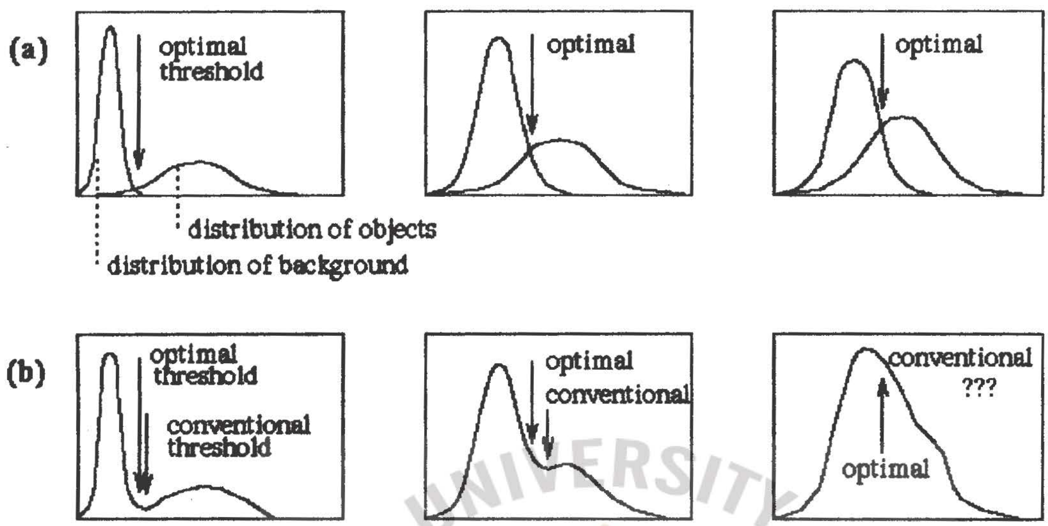

Figure 5.4 ***Grey level histograms approximated by two normal distributions; the threshold is set to give minimum probability of segmentation error: (a) Probability distributions of background and objects, (b) corresponding histograms and optimal threshold.***

Figure 3-1 Illustration of Optimal Thresholding

APPENDIX D

Figure 6-1 From upper left are the bird image, Debbie image, Lenna image, Paolina image, pepper image and Zelda image respectively

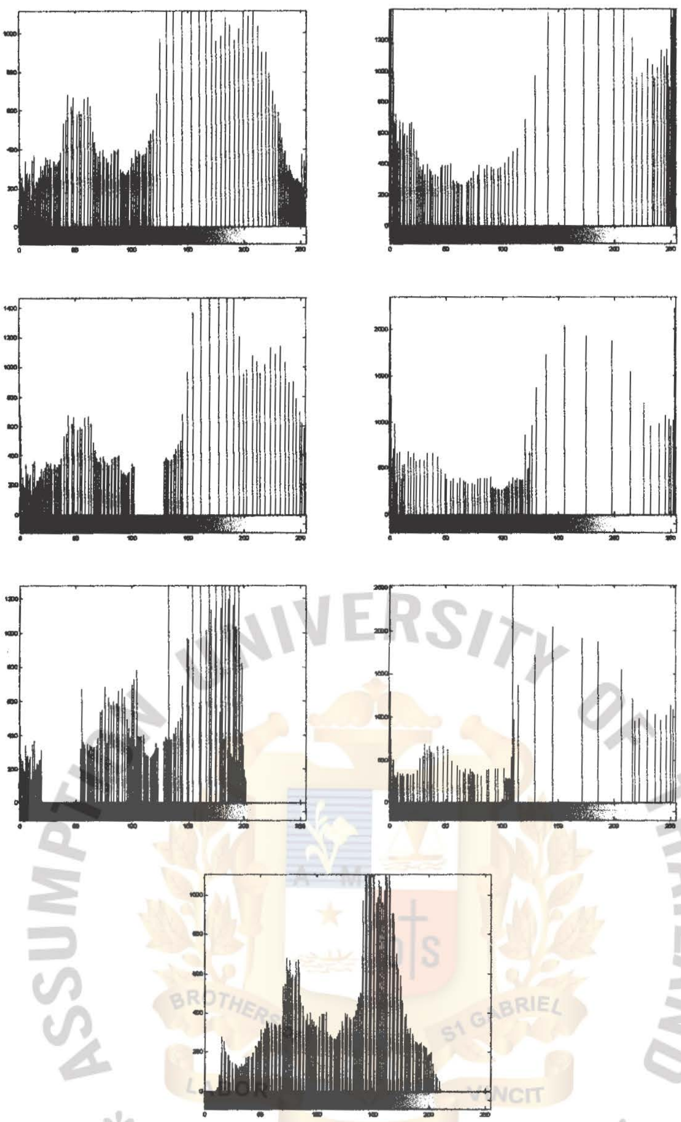

Figure 6-2 from upper left, histogram of bird image after Histogram Equalization, Histogram Specification, HEQBZ_2Z, HSPBZ_2Z, HEQBZ_MZ, HSPBZ_MZ and original image respectively

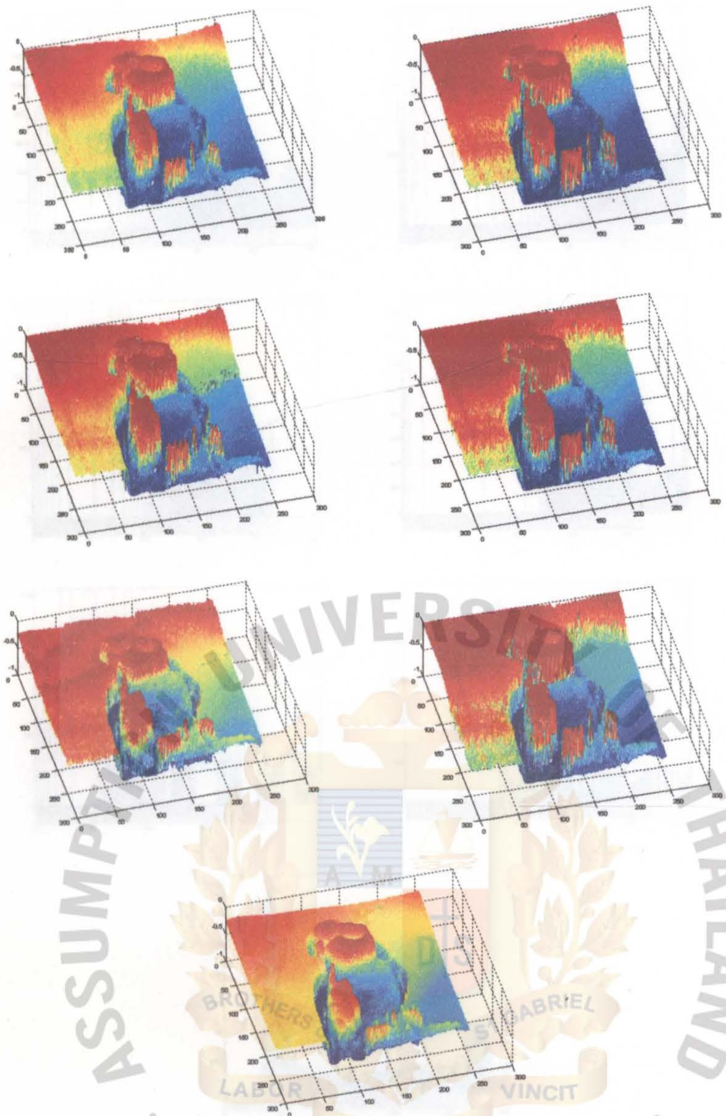

Figure 6-3 From upper left, 3D of bird image after Histogram Equalization, Histogram Specification, HEQBZ_2Z, HSPBZ_2Z, HEQBZ_MZ, HSPBZ_MZ and original image respectively

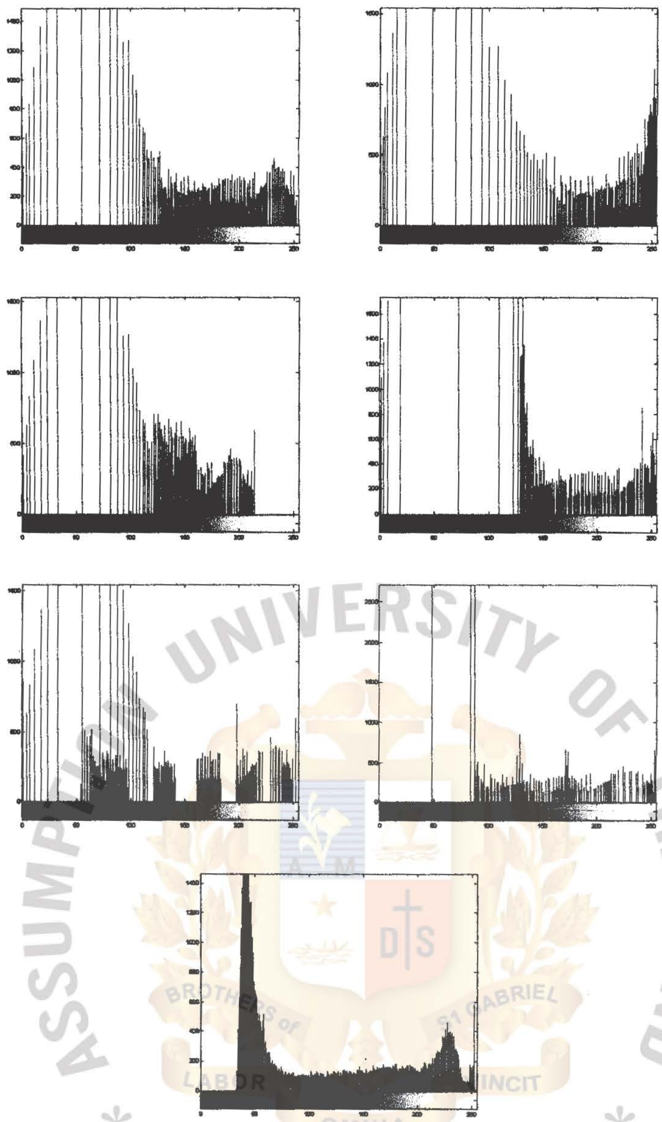

Figure 6-4 From upper left, Histogram of Debbie image after Histogram Equalization, Histogram Specification, HEQBZ_2Z, HSPBZ_2Z, HEQBZ_MZ, HSPBZ_MZ, and original image respectively

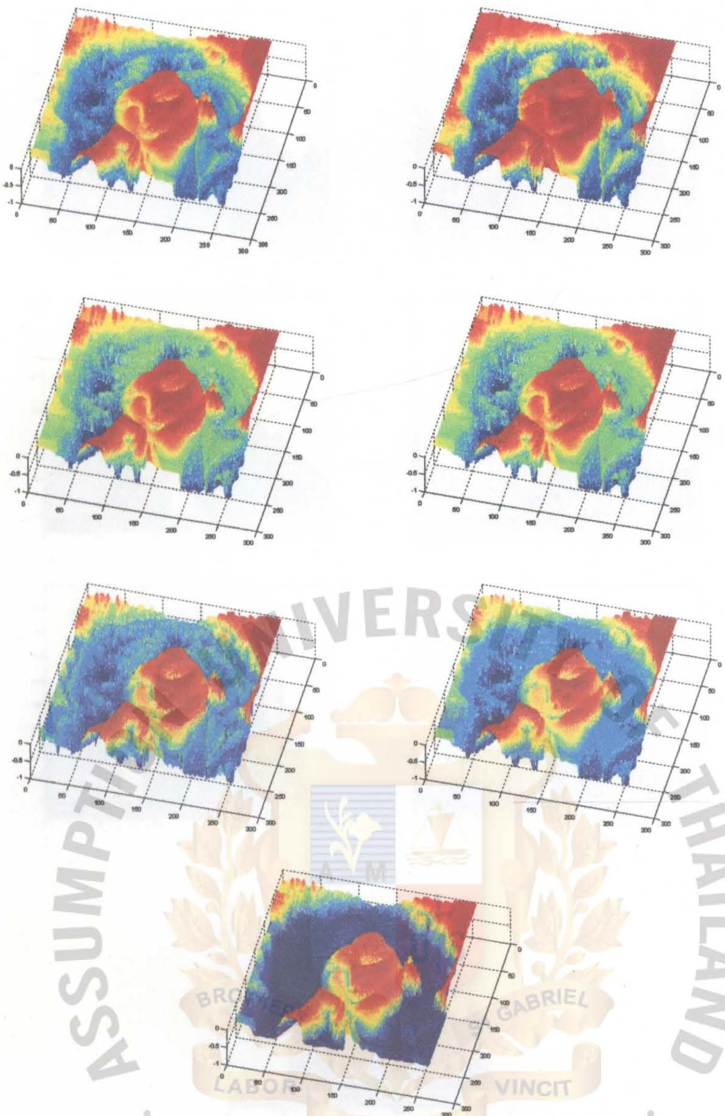

Figure 6-5 From upper left, 3D of Debbie image after Histogram Equalization, Histogram Specification, HEQBZ_2Z, HSPBZ_2Z, HEQBZ_MZ, HSPBZ_MZ, and original image respectively

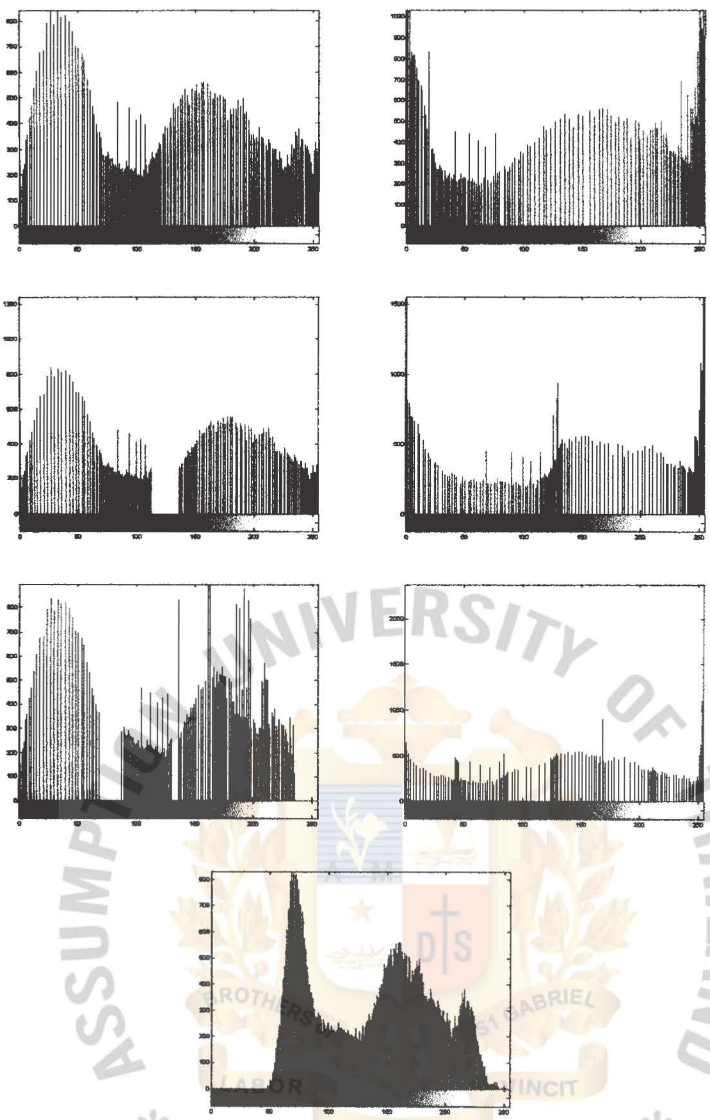

Figure 6-6 From upper left, Histogram of Lenna image after Histogram Equalization, Histogram specification, HEQBZ_2Z, HSPBZ_2Z, HEQBZ_MZ, HSPBZ_MZ, and original respectively

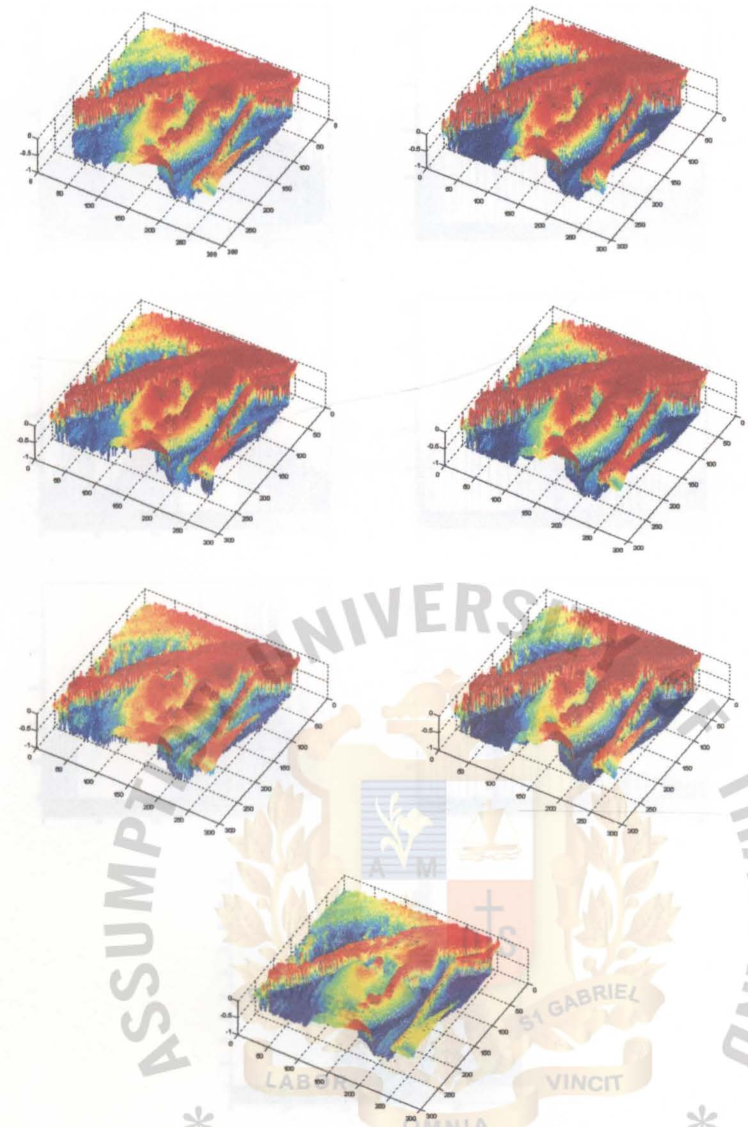

Figure 6-7 From upper left, 3D of Lenna image after Histogram Equalization, Histogram Specification, HEQBZ_2Z, HSPBZ_2Z, HEQBZ_MZ, HSPBZ_MZ, and original image respectively

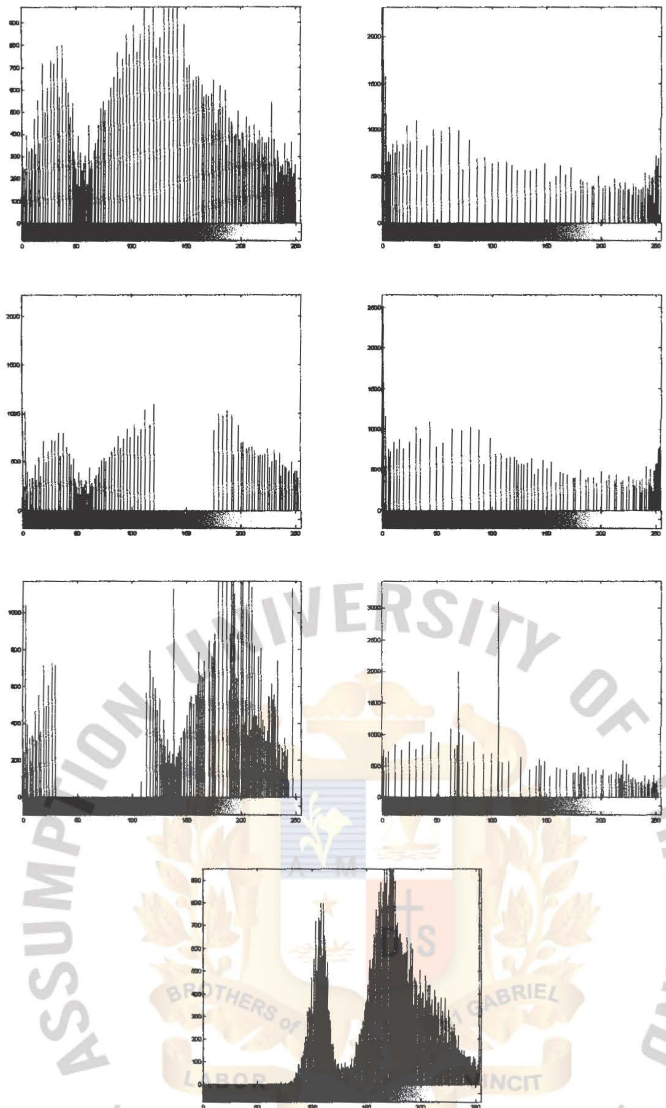

Figure 6-8 From upper left, Histogram of Paolina image after Histogram Equalization, Histogram Specification, HEQBZ_2Z, HSPBZ_2Z, HEQBZ_MZ, HSPBZ_MZ, and original respectively

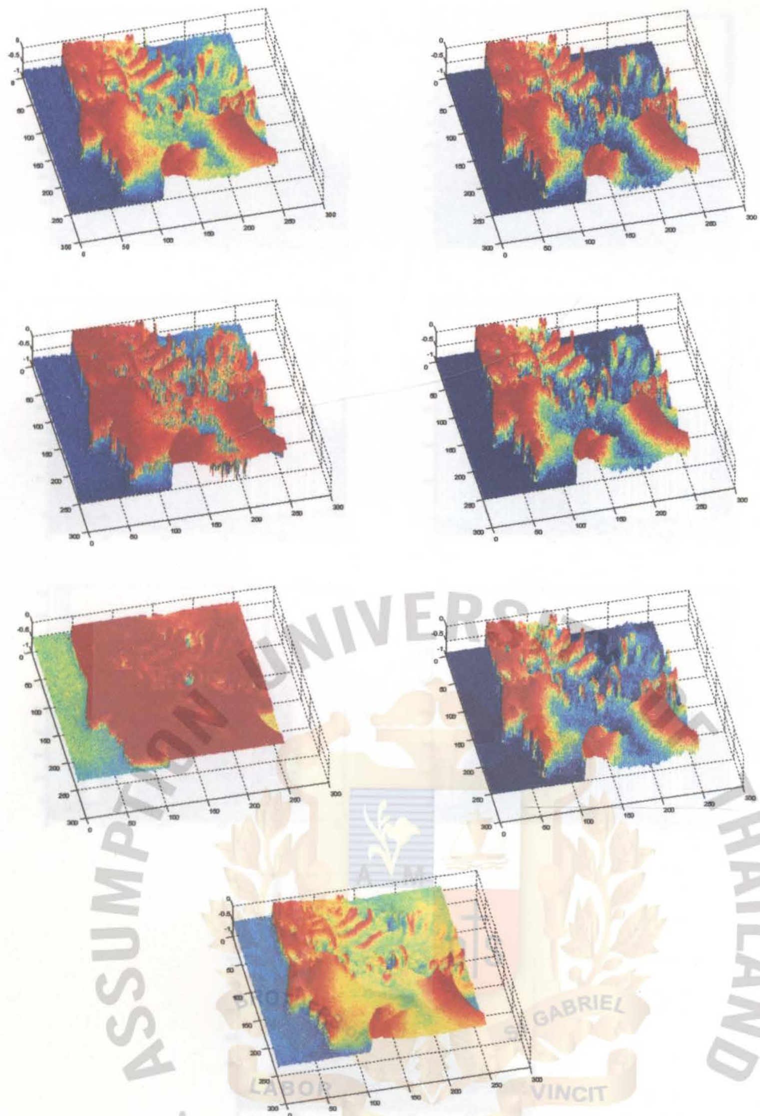

Figure 6-9 From upper left, 3D of Paolina image after Histogram Equalization, Histogram Specification, HEQBZ_2Z, HSPBZ_2Z, HEQBZ_MZ, HSPBZ_MZ, and original image respectively

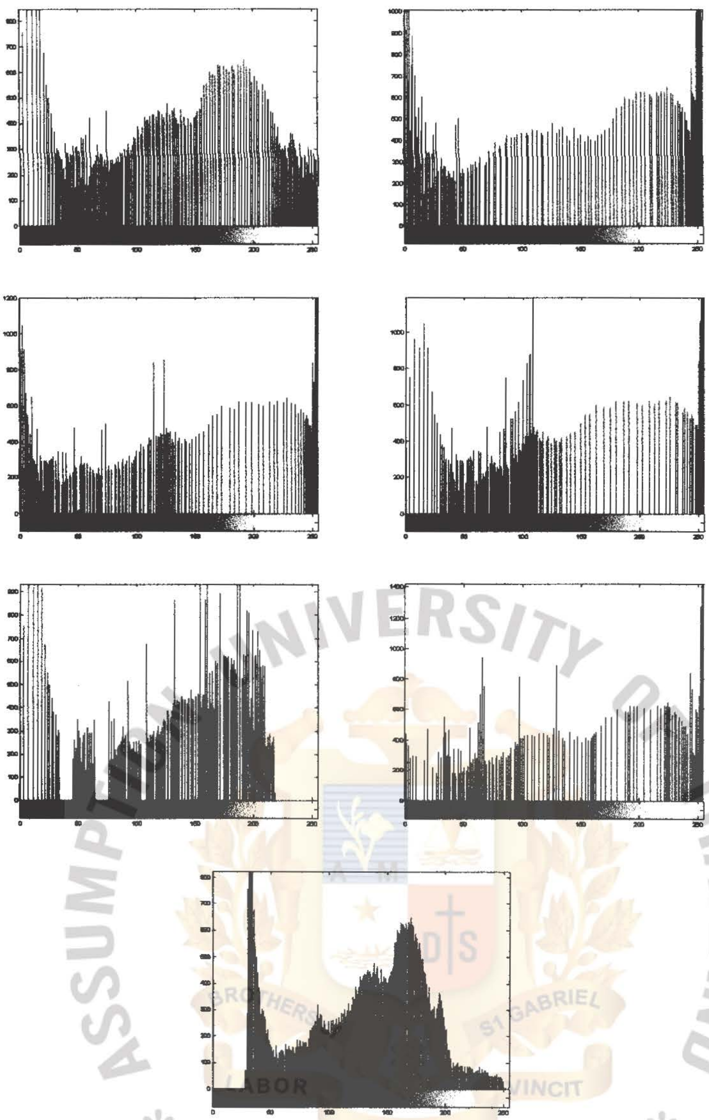

Figure 6-10 From upper left, Histogram of pepper image after Histogram Equalization, Histogram Specification, HEQBZ_2Z, HSPBZ_2Z, HEQBZ_MZ, HSPBZ_MZ, and original respectively

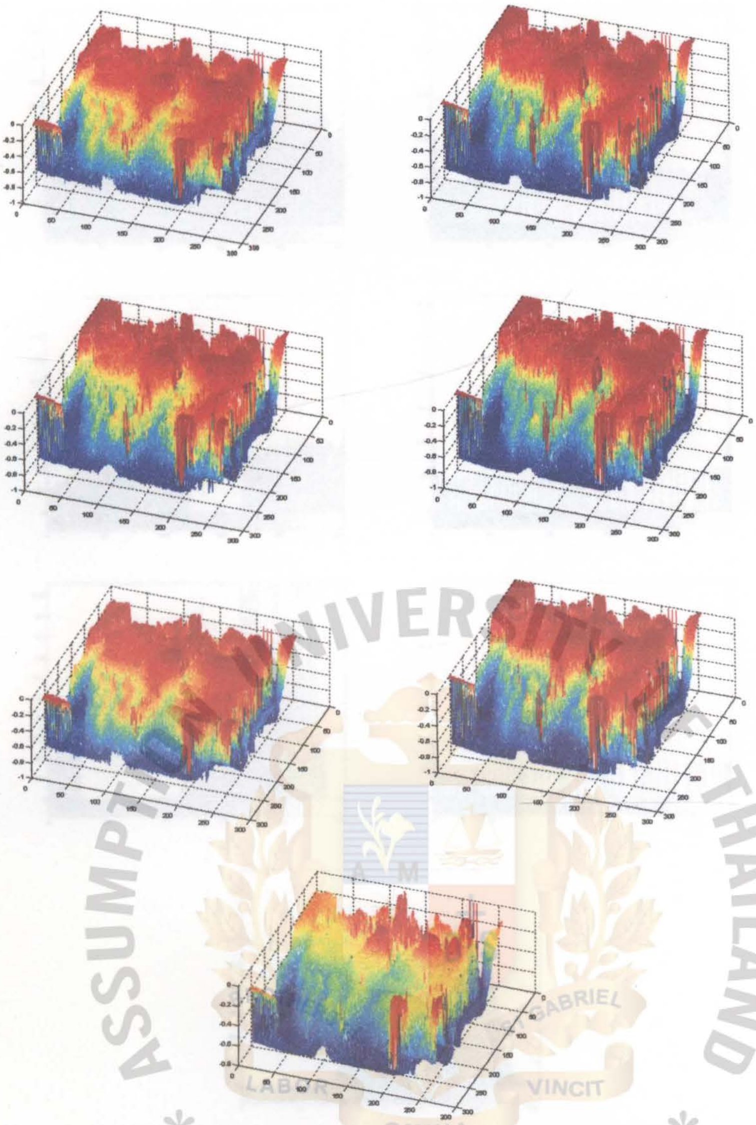

Figure 6-11 From upper left, 3D of pepper image after Histogram Equalization, Histogram Specification, HEQBZ_2Z, HSPBZ_2Z, HEQBZ_MZ, HSPBZ_MZ, and original image respectively

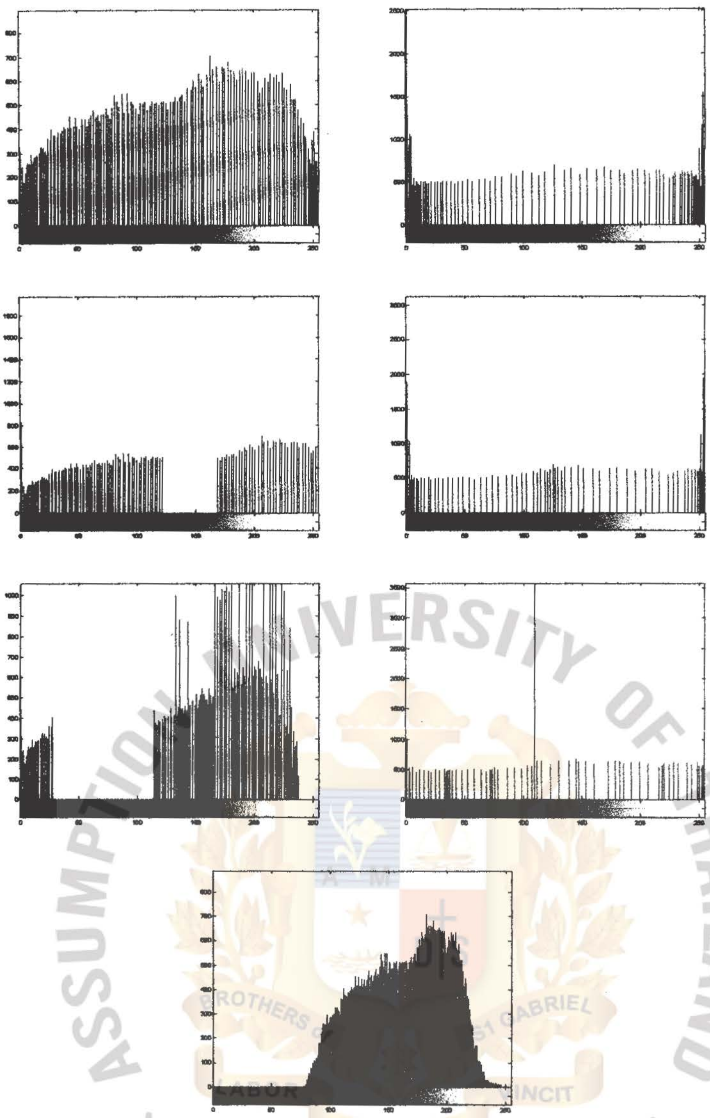

Figure 6-12 From upper left, histogram of Zelda image after Histogram Equalization, Histogram Specification, HEQBZ_2Z, HSPBZ_2Z, HEQBZ_MZ, HSPBZ_MZ, and original respectively

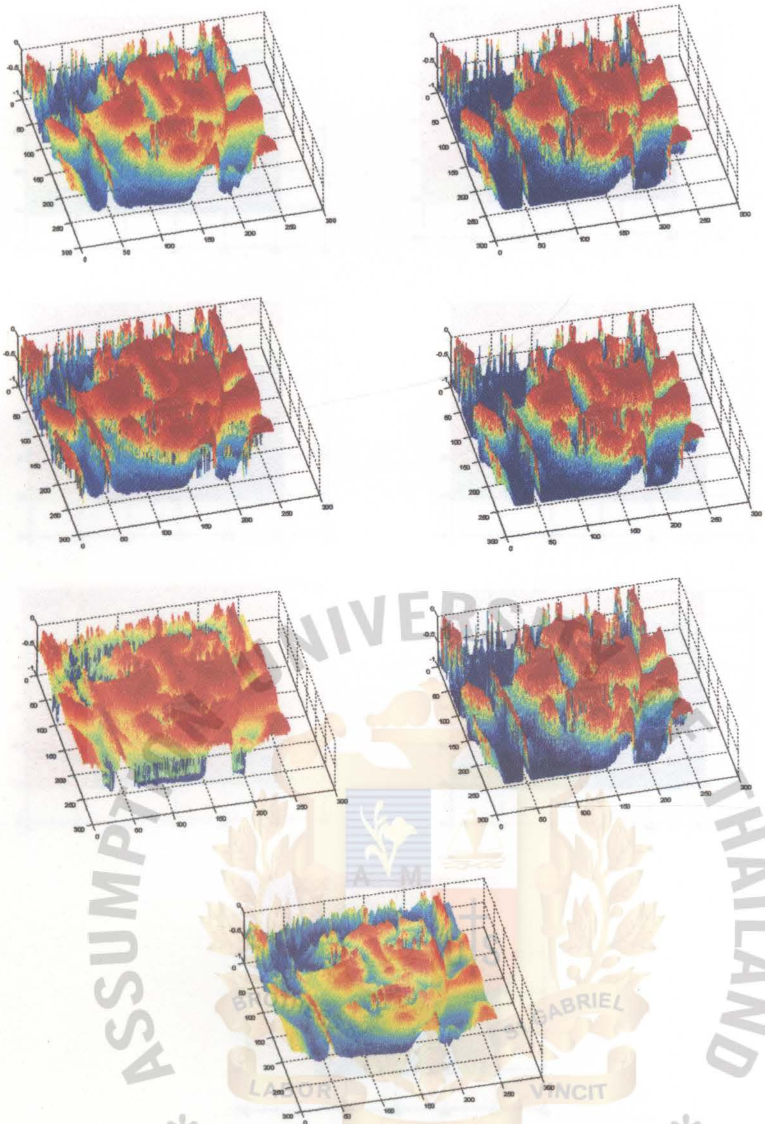

Figure 6-13 From upper left, 3D of Zelda_image after Histogram Equalization, Histogram Specification, HEQBZ_2Z, HSPBZ_2Z, HEQBZ_MZ, HSPBZ_MZ, and original image respectively

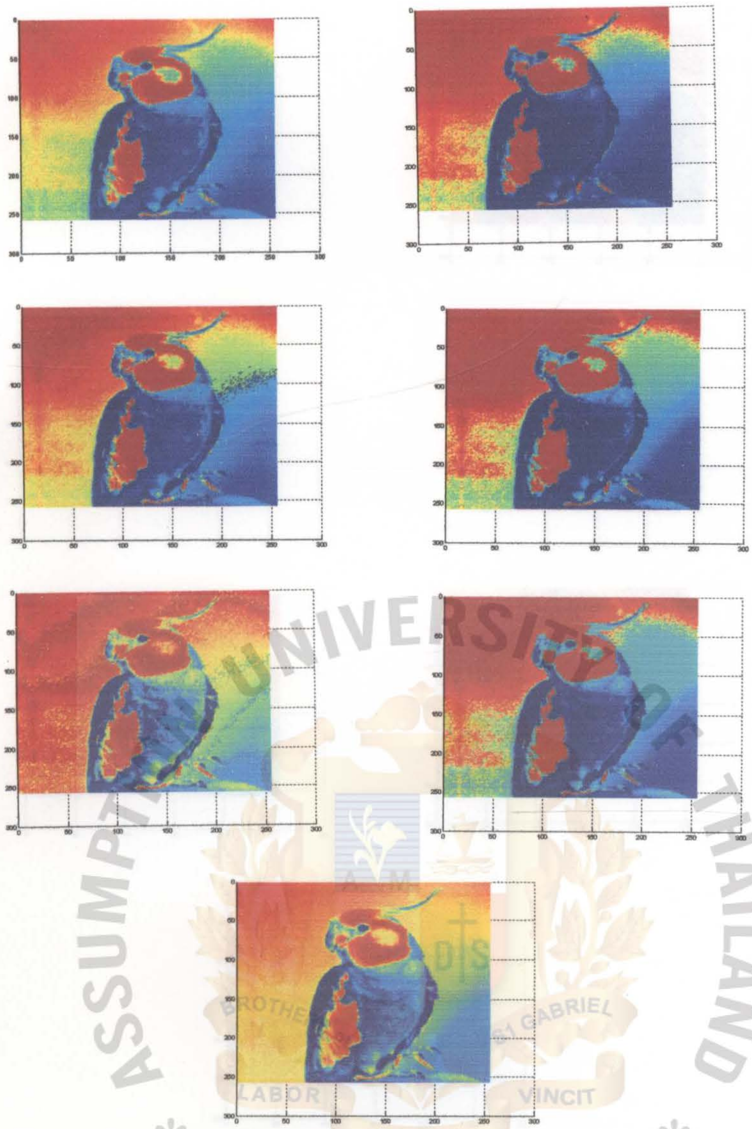

Figure 6-14 From upper left converted 2D from 3D of Bird image after Histogram Equalization, Histogram Specification, HEQBZ_2Z, HSPBZ_2Z, HEQBZ_MZ, HSPBZ_MZ, and original image

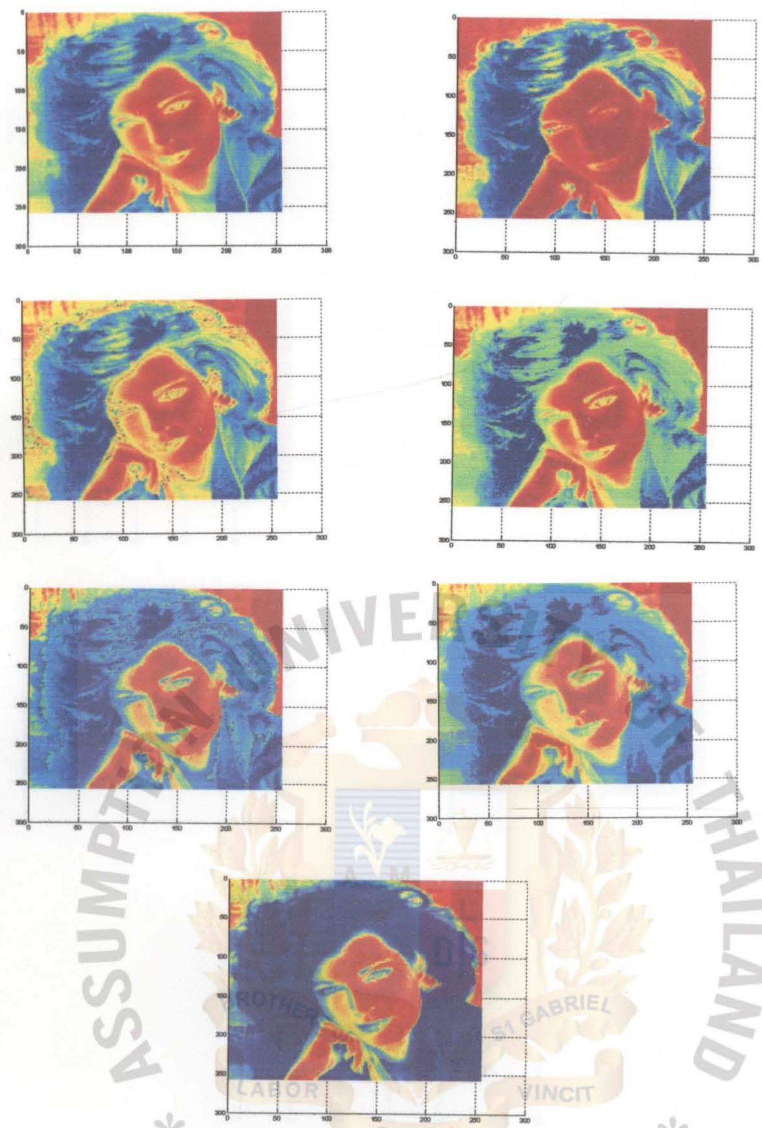

Figure 6-15 From upper left converted 2D from 3D of Debbie image after Histogram Equalization, Histogram Specification, HEQBZ_2Z, HSPBZ_2Z, HEQBZ_MZ, HSPBZ_MZ, and original image

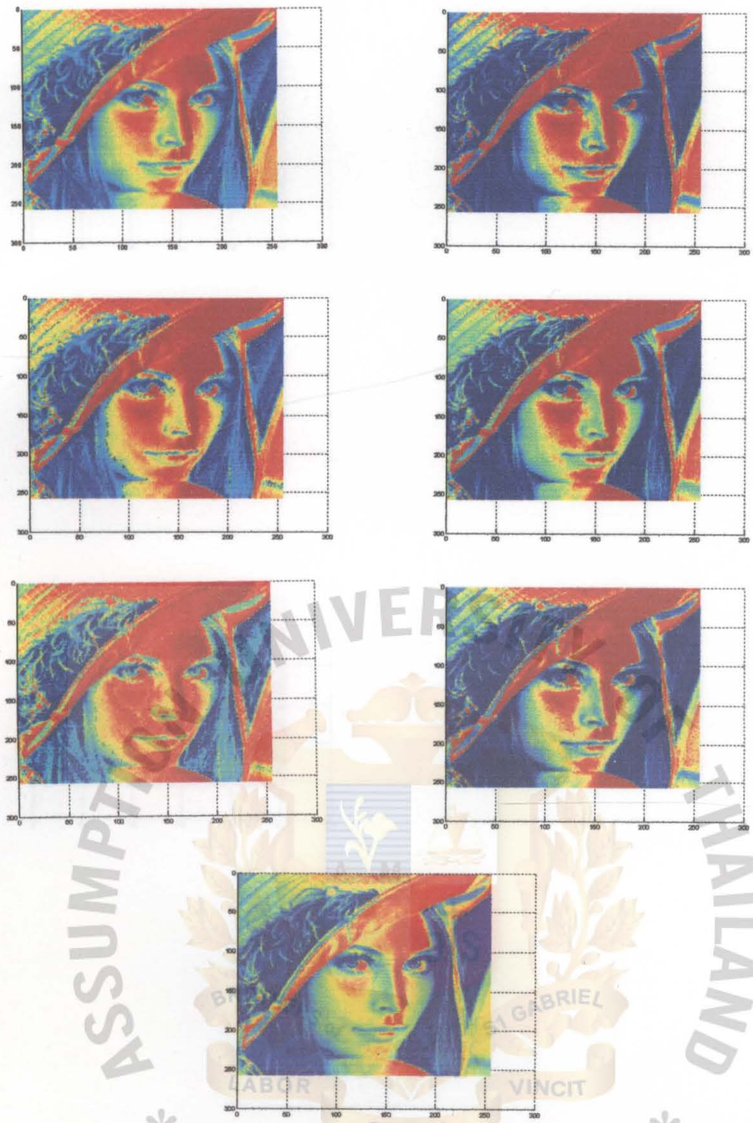

Figure 6-16 From upper left converted 2D from 3D of Lenna image after Histogram Equalization, Histogram Specification, HEQBZ_2Z, HSPBZ_2Z, HEQBZ_MZ, HSPBZ_MZ, and original image

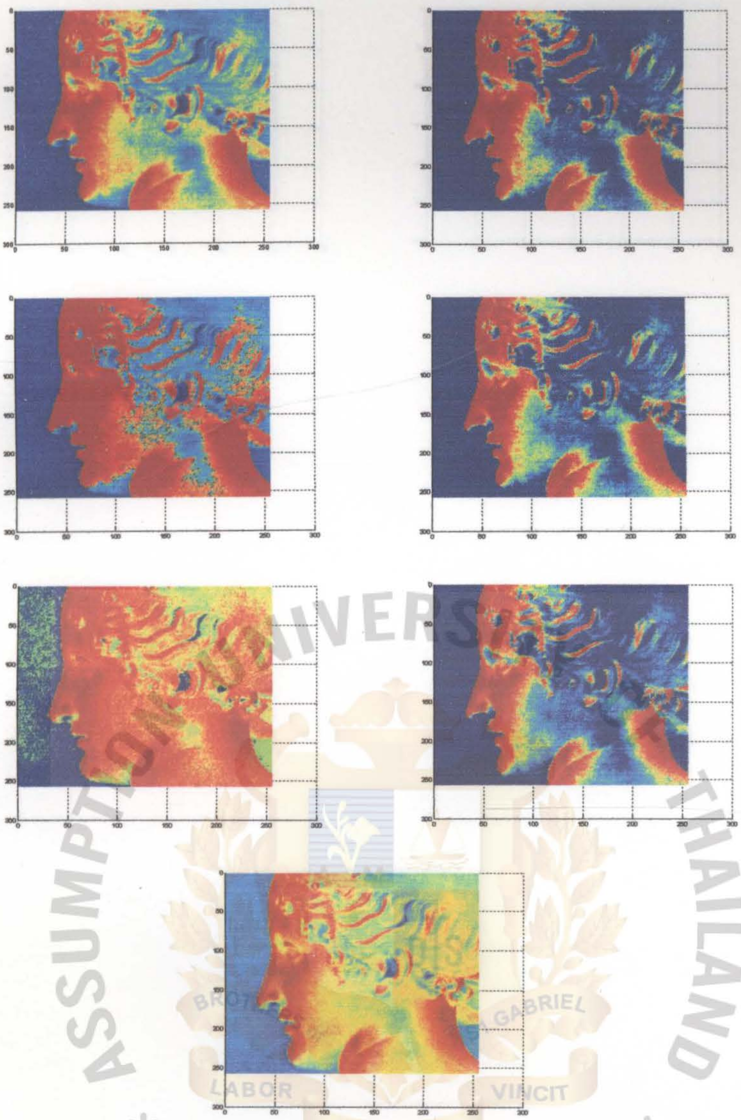

Figure 6-17 From upper left converted 3D from 2D of Paolina image after Histogram Equalization, Histogram Specification, HEQBZ_2Z, HSPBZ_2Z, HEQBZ_MZ, HSPBZ_MZ, and original image

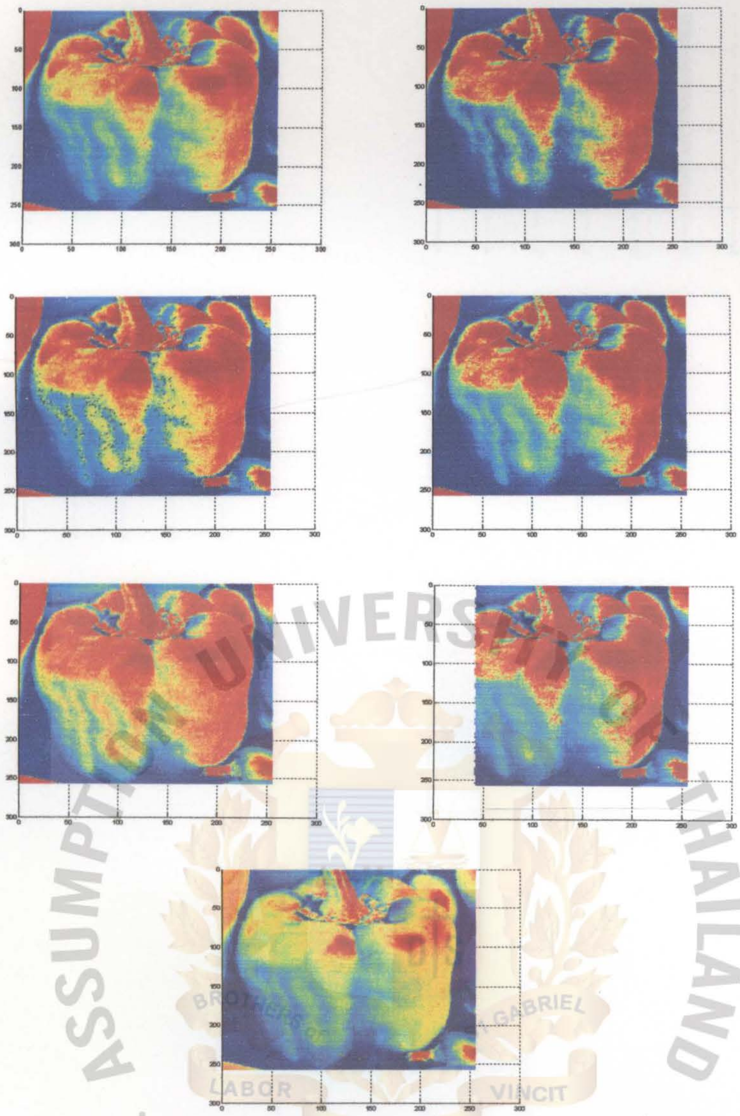

Figure 6-18 From upper left converted 2D from 3D of Pepper image after Histogram Equalization, Histogram Specification, HEQBZ_2Z, HSPBZ_2Z, HEQBZ_MZ, HSPBZ_MZ, and original image

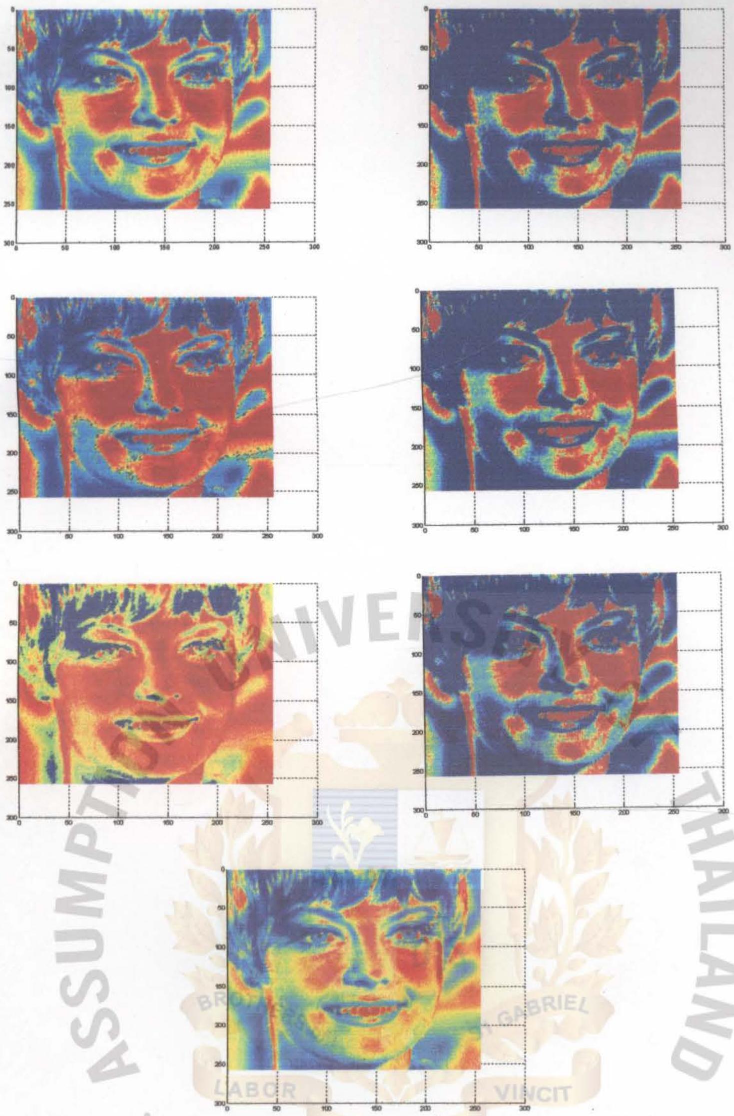

Figure 6-19 From upper left converted 2D from 3D of Zelda image after Histogram Equalization, Histogram Specification, HEQBZ_2Z, HSPBZ_2Z, HEQBZ_MZ, HSPBZ_MZ, and original image